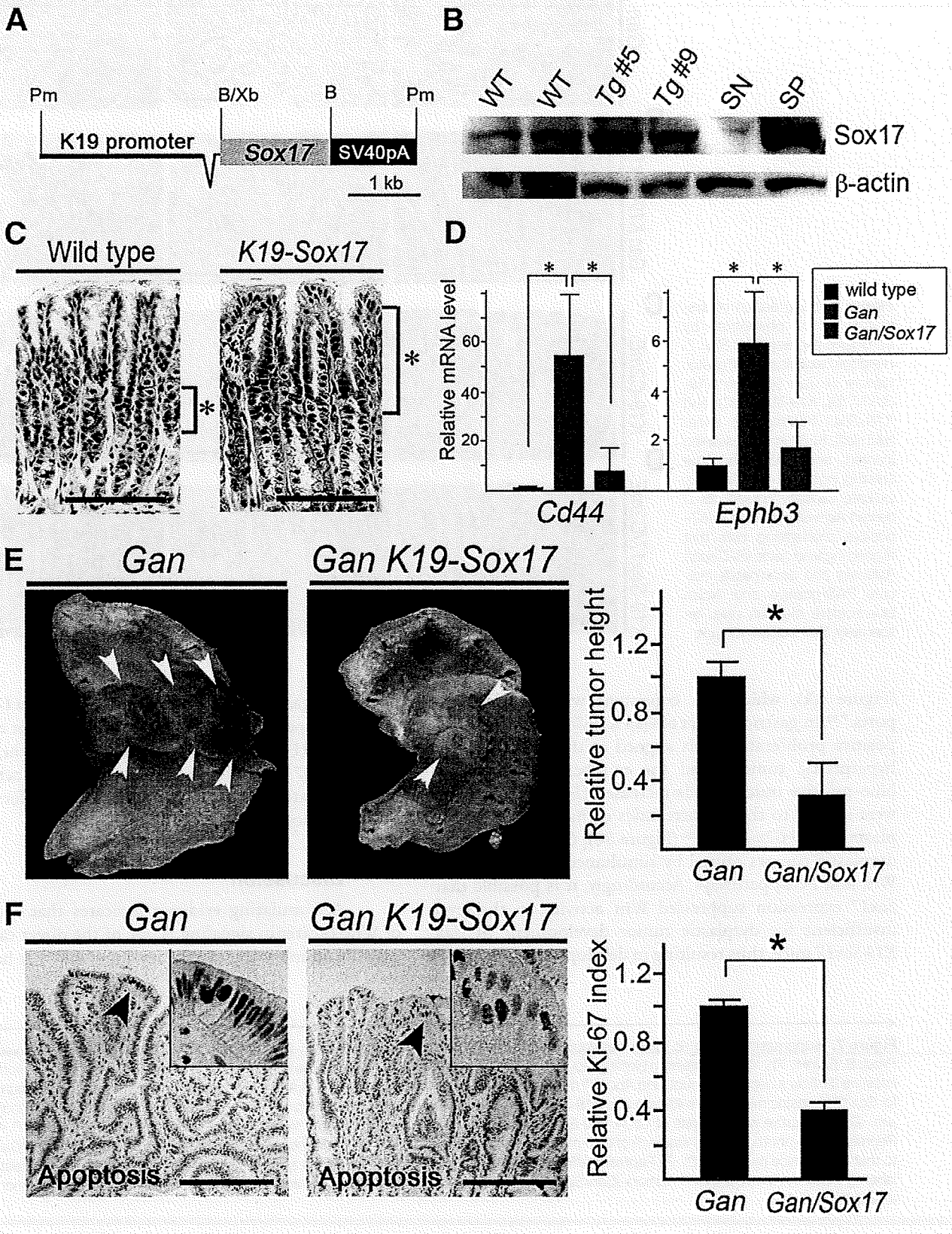
A
Pm
B/Xb
B
Pm
K19 promoter
Sox17
SV40pA
1 kb
B
WT
WT
Tg #5
Tg #9
SN
SP
Sox17
β-actin
C
Wild type
K19-Sox17
D
Relative mRNA level
wild type
Gan
Gan/Sox17
Cd44
Ephb3
E
Gan
Gan K19-Sox17
Relative tumor height
Gan
Gan/Sox17
F
Gan
Gan K19-Sox17
Apoptosis
Apoptosis
Relative Ki-67 index
Gan
Gan/Sox17

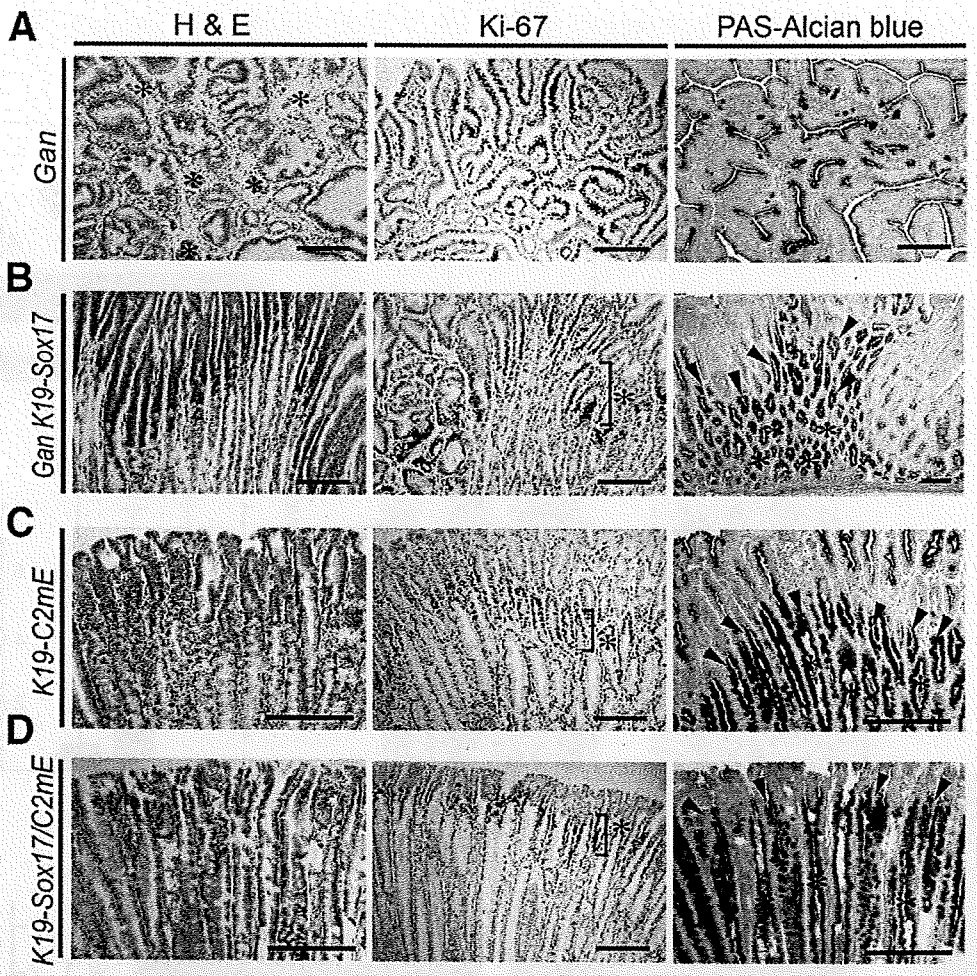

Figure 8. Suppression of dysplastic tumor phenotype by transgenic expression of *Sox17*. Histologic examination of gastric tumors in *Gan* (*A*), *Gan K19-Sox17* (*B*), *K19-C2mE* (*C*), and *K19-Sox17/C2mE* (*D*) mice. H&E (*left*), Ki-67 immunostaining (*center*), and PAS-Alcian blue staining (*right*). (*A left*) *Asterisks* indicate capillary vessels. (*B–D center*) *Asterisks* indicate Ki-67–positive proliferating cells that aligned in gland neck. (*B–D right*) *Asterisks* and *arrowheads* indicate PAS-positive and Alcian blue-positive mucous cells, respectively. Bars indicate 100 μm.

(Figure 8*A*), which was consistent with previous reports.[7,31] In gastric tumors of *Gan K19-Sox17* mice, Ki-67–positive proliferating cells aligned at the gland neck of hyperplastic tumors, and the number of PAS-Alcian blue–positive mucous cells increased (Figure 8*B*), which were similar to the characteristics of metaplastic hyperplasia of *K19-C2mE* mice[29] (Figure 8*C*). *Gan* mice develop dysplastic tumors caused by simultaneous activation of Wnt and PGE_2 pathways. Accordingly, it is possible that *Sox17* expression suppressed Wnt activity to the level insufficient for dysplastic tumor development in *Gan K19-Sox17* mice, thus resulting in development of a PGE_2-dependent gastric phenotype. Moreover, *K19-Sox17/C2mE* mice developed metaplastic hyperplasia but not dysplastic tumors (Figure 8*D*), thus indicating that the induction of *Sox17* and PGE_2 pathways without the activation of Wnt/β-catenin signaling is not sufficient for gastric tumor development.

Discussion

Accumulating evidence indicates that activation of Wnt/β-catenin signaling is one of the direct causes of gastric and intestinal tumor development.[4–7] It has been

Figure 7. Suppression of gastric tumor development by transgenic expression of *Sox17*. (*A*) Schematic construction of transgenic vector. Pm, *Pme*I; B, *Bam*HI; Xb, *Xba*I. (*B*) Western blotting results of Sox17 in gastric mucosa of wild-type (WT), *K19-Sox17* (Tg) line no. 5 and no. 9, normal small intestine (SN) as a negative control, and $Apc^{\Delta 716}$ mouse polyps (SP) as a positive control. β-Actin was used for internal control. (*C*) Immunostaining for Sox17 in gastric mucosa of wild-type and *K19-Sox17* mice. *Asterisks* indicate localization of Sox17-expressing epithelial cells. *Bars* indicate 100 μm. (*D*) The relative mRNA levels of *Cd44* and *Ephb3* in *Gan* (*red*) and *Gan K19-Sox17* mice (*blue*) to the wild-type level (*black*). $^*P < .05$. (*E*) Representative photographs of stomach of *Gan* mouse and *Gan K19-Sox17* mouse, and the relative tumor height in *Gan K19-Sox17* (*Gan/Sox17*) to that in *Gan* mice (mean ± SD). (*F*) Representative photographs for apoptotic cells in *Gan* and *Gan K19-Sox17* mouse tumors, and relative Ki-67 labeling index in *Gan K19-Sox17* tumors (*Gan/Sox17*) to that in *Gan* mouse tumors. *Arrowheads* indicate apoptotic cells on the tumor surface. (*E* and *F*) $^*P < .05$.

shown that the expression of several *Sox* family genes, including *Sox2*, *Sox9*, and *Sox17* are induced by Wnt/β-catenin signaling.[32–34] In the present study, we found that activation of Wnt signaling causes *Sox17* expression in gastric cancer cells and that *Sox17* is induced in benign gastric tumors. Because Sox17 antagonizes Wnt/β-catenin signaling, it is thus conceivable that the Wnt activation level in the early stage of tumorigenesis is partially suppressed by Sox17 but is sufficient for benign tumor development. Importantly, transgenic expression of *Sox17* in the *Gan* mouse stomach suppressed dysplastic tumor formation. Suppression of the dysplastic phenotype of *Gan K19-Sox17* mouse tumors is possibly caused by repression of Wnt/β-catenin signaling. Namely, overexpression of *Sox17* suppresses Wnt/β-catenin signaling activity to the level insufficient for tumor formation. Therefore, it is possible that *Sox17* induction level at the early stage of tumorigenesis is strictly regulated to maintain the Wnt/β-catenin activity for dysplastic tumor development.

However, *Sox17* expression is dramatically suppressed in most human gastric cancer cells possibly through promoter methylation, which may result in an increase of Wnt/β-catenin signaling activity in comparison to that in benign tumors. We also confirmed *Sox17* down-regulation in human colon cancer tissues. Recently, it has been suggested that promotion of Wnt/β-catenin signaling is required for malignant progression of colon cancer.[8] Consistently, we found that *Sox17* transfection reduced the colony formation efficiency in gastric cancer cells. Accordingly, it is possible that down-regulation of *Sox17* contributes to malignant behavior through promotion of Wnt/β-catenin signaling both in the stomach and colon. Therefore, induction of tumor suppressor *Sox17* at the early stage of tumorigenesis can be considered as a self-protection system against malignant tumor development.

In the present study, we found drastic changes of *Sox17* expression during the course of intestinal tumorigenesis in $Apc^{\Delta 716}$ and *cis-*$Apc^{\Delta 716}$ *Smad4* mice. The previous genetic studies indicate that mutations in both *Apc* and *Smad4* cause malignant tumor development in the intestine.[28,35] However, because *Sox17* down-regulation was tightly associated with invasive tumor phenotype in *cis-*$Apc^{\Delta 716}$ *Smad4* mice, it is conceivable that *Sox17* suppression in addition to *Apc* and *Smad4* mutations is required for malignant progression to adenocarcinoma. Because *Sox17* down-regulation was found only in the *cis-*$Apc^{\Delta 716}$ *Smad4* mouse tumors but not in $Apc^{\Delta 716}$ polyps, it is possible that disruption of the transforming growth factor-β pathway contributes to suppression of *Sox17* expression.

Sox17 is required for definitive endoderm development, which gives rise to gut formation.[20,21,26] Moreover, it has been shown that β-catenin is also essential for definitive endoderm formation.[36] We have shown here that *Sox17* continuously expresses in the stomach and intestine during organogenesis. Importantly, Wnt signaling is also activated in the gastrointestinal tract of embryonic and neonatal stages. These results suggest that cooperation of Sox17 and Wnt/β-catenin pathway plays a role also in the morphogenesis of the gastrointestinal tract. Dysregulation of morphogen signals, such as Notch, Hh, or Wnt, in adult tissues often results in pathologic conditions, such as tumor development.[37] We herein show that the Sox17 target genes, which encode molecules that play a role in the definitive endoderm development, are induced in *Gan* mouse tumors. Although *Sox17* induction is not sufficient for tumorigenesis, as found in *K19-Sox17* or *K19-Sox17/C2mE* mice, it is possible that the activation of both Wnt- and Sox17-target molecules cooperatively causes gastric tumor development.

In conclusion, *Sox17* is induced at the early stage of tumorigenesis caused by Wnt/β-catenin activation, and Sox17 together with Wnt/β-catenin signaling may play a role in tumor development through induction of target genes. At the same time, Sox17 may play a preventive role against malignant progression through repression of Wnt activity. Therefore, it is conceivable that induction and down-regulation of *Sox17* expression is important for tumor initiation and malignant progression, respectively, in the course of gastrointestinal tumorigenesis.

Supplementary Data

Note: To access the supplementary material accompanying this article, visit the online version of *Gastroenterology* at www.gastrojournal.org, and at doi: 10.1053/j.gastro.2009.06.041.

References

1. Nusse R. Wnt signaling in disease and in development. Cell Res 2005;15:28–32.
2. Korinek V, Barker N, Moerer P, et al. Depletion of epithelial stem-cell compartments in the small intestine of mice lacking Tcf-4. Nat Genet 1998;19:379–383.
3. van de Wetering M, Sancho E, Verweij C, et al. The β-catenin/TCF-4 complex imposes a crypt progenitor phenotype on colorectal cancer cells. Cell 2002;111:241–250.
4. Clements WM, Wang J, Sarnaik A, et al. β-Catenin mutation is a frequent cause of Wnt pathway activation in gastric cancer. Cancer Res 2002;62:3503–3506.
5. Fodde R, Smits R, Clevers H. *APC*, signal transduction and genetic instability in colorectal cancer. Nat Rev Cancer 2001;1:55–67.
6. Oshima M, Oshima H, Kitagawa K, et al. Loss of *Apc* heterozygosity and abnormal tissue building in nascent intestinal polyps in mice carrying a truncated *Apc* gene. Proc Natl Acad Sci U S A 1995;92:4482–4486.
7. Oshima H, Matsunaga A, Fujimura T, et al. Carcinogenesis in mouse stomach by simultaneous activation of the Wnt signaling and prostaglandin E_2 pathway. Gastroenterology 2006;131:1086–1095.
8. Fodde R, Brabletz T. Wnt/β-catenin signaling in cancer stemness and malignant behavior. Curr Opin Cell Biol 2007;19:150–158.

9. Yang L, Lin C, Liu Z-R. p68 RNA helicase mediates PDGF-induced epithelial mesenchymal transition by displacing Axin from β-catenin. Cell 2006;127:139–155.
10. Rasola A, Fassetta M, De Bacco F, et al. A positive feedback loop between hepatocyte growth factor receptor and β-catenin sustains colorectal cancer cell invasive growth. Oncogene 2007; 26:1078–1087.
11. Oguma K, Oshima H, Aoki M, et al. Activated macrophages promote Wnt signalling through tumour necrosis factor-α in gastric tumour cells. EMBO J 2008;27:1671–1681.
12. Taketo MM. Shutting down Wnt signal-activated cancer. Nat Genet 2004;36:320–322.
13. Suzuki H, Watkins DN, Jair K-W, et al. Epigenetic inactivation of *SFRP* genes allows constitutive WNT signaling in colorectal cancer. Nat Genet 2004;36:417–422.
14. Nojima M, Suzuki H, Toyota M, et al. Frequent epigenetic inactivation of *SFRP* genes and constitutive activation of Wnt signaling in gastric cancer. Oncogene 2007;26:4699–4713.
15. Zhang C, Basta T, Jensen ED, et al. The β-catenin/VegT-regulated early zygotic gene *Xnr5* is a direct target of SOX3 regulation. Development 2003;130:5609–5624.
16. Takash W, Cañizares J, Bonneaud N, et al. SOX7 transcription factor: sequence, chromosomal localisation, expression, transactivation and interference with Wnt signalling. Nucleic Acid Res 2001;29:4274–4283.
17. Akiyama H, Lyons JP, Mori-Akiyama Y, et al. Interactions between Sox9 and β-catenin control chondrocyte differentiation. Genes Dev 2004;18:1072–1087.
18. Zorn AM, Barish GD, Williams BO, et al. Regulation of Wnt signaling by Sox proteins: XSox17α/β and XSox3 physically interact with β-catenin. Mol Cell 1999;4:487–498.
19. Gubbay J, Collignon J, Koopman P, et al. A gene mapping to the sex-determining region of the mouse Y chromosome is a member of a novel family of embryonically expressed genes. Nature 1990; 346:245–250.
20. Kanai-Azuma M, Kanai Y, Gad JM, et al. Depletion of definitive gut endoderm in *Sox17*-null mutant mice. Development 2002;129: 2367–2379.
21. Séguin CA, Draper JS, Nagy A, et al. Establishment of endoderm progenitors by SOX transcription factor expression in human embryonic stem cells. Cell Stem Cell 2008;3:182–195.
22. Zhang W, Glöckner SC, Guo M, et al. Epigenetic inactivation of the canonical Wnt antagonist SRY-box containing gene 17 in colorectal cancer. Cancer Res 2008;68:2764–2772.
23. Sinner D, Kordich JJ, Spence JR, et al. Sox17 and Sox4 differentially regulate β-catenin/T-cell factor activity and proliferation of colon carcinoma cells. Mol Cell Biol 2007;27:7802–7815.
24. Oshima H, Oshima M, Kobayashi M, et al. Morphological and molecular processes of polyp formation in $Apc^{\Delta 716}$ knockout mice. Cancer Res 1997;57:1644–1649.
25. Harada N, Tamai Y, Ishikawa T, et al. Intestinal polyposis in mice with a dominant stable mutation of the β-catenin gene. EMBO J 1999;18:5931–5942.
26. Tam PPL, Kanai-Azuma M, Kanai Y. Early endoderm development in vertebrates: lineage differentiation and morphogenetic function. Curr Opin Genet Dev 2003;13:393–400.
27. Sinner D, Rankin S, Lee M, et al. Sox17 and β-catenin cooperate to regulate the transcription of endodermal genes. Development 2004;131:3069–3080.
28. Takaku K, Oshima M, Miyoshi H, et al. Intestinal tumorigenesis in compound mutant mice of both *Dpc4* (*Smad4*) and *Apc* gene. Cell 1998;92:645–656.
29. Oshima H, Oshima M, Inaba K, et al. Hyperplastic gastric tumors induced by activated macrophages in COX-2/mPGES-1 transgenic mice. EMBO J 2004;23:1669–1678.
30. Leung SY, Chen X, Chu KM, et al. Phospholipase A2 group IIA expression in gastric adenocarcinoma is associated with prolonged survival and less frequent metastasis. Proc Natl Acad Sci U S A 2002;99:16203–16208.
31. Guo X, Oshima H, Kitamura T, et al. Stromal fibroblasts activated by tumor cells promote angiogenesis in mouse gastric cancer. J Biol Chem 2008;283:19864–19871.
32. Blache P, van de Wetering M, Duluc I, et al. SOX9 is an intestine crypt transcription factor, is regulated by the Wnt pathway, and represses the CDX2 and MUC2 genes. J Cell Biol 2004;166: 37–47.
33. Van Raay TJ, Moore KB, Iordanova I, et al. Frizzled 5 signaling governs the neural potential of progenitors in the developing Xenopus retina. Neuron 2005;46:23–36.
34. Sansom OJ, Reed KR, Hayes AJ, et al. Loss of Apc in vivo immediately perturbs Wnt signaling, differentiation, and migration. Genes Dev 2004;18:1385–1390.
35. Kitamura T, Kometani K, Hashida H, et al. SMAD4-deficient intestinal tumors recruit CCR1+ myeloid cells that promote invasion. Nat Genet 2007;39:467–475.
36. Lickert H, Kutsch S, Kanzler B, et al. Formation of multiple hearts in mice following deletion of β-catenin in the embryonic endoderm. Dev Cell 2002;3:171–181.
37. Gregorieff A, Clevers H. Wnt signaling in the intestinal epithelium: from endoderm to cancer. Genes Dev 2005;19:877–890.

Received February 5, 2009. Accepted June 11, 2009.

Reprint requests

Address requests for reprints to: Masanobu Oshima, DVM, PhD, Division of Genetics, Cancer Research Institute, Kanazawa University, 13-1 Takara-machi, Kanazawa, 920-0934 Japan. e-mail: oshimam@kenroku.kanazawa-u.ac.jp; fax: (81) 76-234-4519.

Acknowledgments

The authors thank Manami Watanabe for excellent technical assistance.

Conflicts of interest

The authors disclose no conflicts.

Funding

Supported by Grants-in-Aid from the Ministry of Education, Culture, Sports, Science, and Technology of Japan and by the Ministry of Health, Labour, and Welfare of Japan (to M.O.).

OPEN ACCESS Freely available online

PLoS one

Generation of Knockout Rats with X-Linked Severe Combined Immunodeficiency (X-SCID) Using Zinc-Finger Nucleases

Tomoji Mashimo[1]*, Akiko Takizawa[1], Birger Voigt[1], Kazuto Yoshimi[1], Hiroshi Hiai[2], Takashi Kuramoto[1], Tadao Serikawa[1]

1 Institute of Laboratory Animals, Graduate School of Medicine, Kyoto University, Kyoto, Japan, 2 Shiga Medical Center for Adult Disease, Moriyama, Japan

Abstract

Background: Although the rat is extensively used as a laboratory model, the inability to utilize germ line-competent rat embryonic stem (ES) cells has been a major drawback for studies that aim to elucidate gene functions. Recently, zinc-finger nucleases (ZFNs) were successfully used to create genome-specific double-stranded breaks and thereby induce targeted gene mutations in a wide variety of organisms including plants, drosophila, zebrafish, etc.

Methodology/Principal Findings: We report here on ZFN-induced gene targeting of the rat interleukin 2 receptor gamma (*Il2rg*) locus, where orthologous human and mouse mutations cause X-linked severe combined immune deficiency (X-SCID). Co-injection of mRNAs encoding custom-designed ZFNs into the pronucleus of fertilized oocytes yielded genetically modified offspring at rates greater than 20%, which possessed a wide variety of deletion/insertion mutations. ZFN-modified founders faithfully transmitted their genetic changes to the next generation along with the severe combined immune deficiency phenotype.

Conclusions and Significance: The efficient and rapid generation of gene knockout rats shows that using ZFN technology is a new strategy for creating gene-targeted rat models of human diseases. In addition, the X-SCID rats that were established in this study will be valuable *in vivo* tools for evaluating drug treatment or gene therapy as well as model systems for examining the treatment of xenotransplanted malignancies.

Citation: Mashimo T, Takizawa A, Voigt B, Yoshimi K, Hiai H, et al. (2010) Generation of Knockout Rats with X-Linked Severe Combined Immunodeficiency (X-SCID) Using Zinc-Finger Nucleases. PLoS ONE 5(1): e8870. doi:10.1371/journal.pone.0008870

Editor: Ellen A. A. Nollen, University Medical Center Groningen, Netherlands

Received November 12, 2009; **Accepted** January 4, 2010; **Published** January 25, 2010

Funding: This study was supported in part by a grant-in-aid for cancer research from the Ministry of Health, Labour, and Welfare. The funders had no role in study design, data collection and analysis, decision to publish, or preparation of the manuscript.

Competing Interests: The authors have declared that no competing interests exist.

* E-mail: tmashimo@anim.med.kyoto-u.ac.jp

Introduction

Although several strategies are available for producing a wide variety of genomic alterations in the mouse, the same cannot be said of the rat. Rat ES cells [1,2] and induced pluripotent stem cells (iPS) [3,4] are available, but the culture conditions for these cells and the methodology for inducing homologous recombination are imperfect [5]. Rat spermatogonial stem cells (SSC) have also been isolated and cultivated *in vitro* but their yield proved unsatisfactory in terms of their ability to undergo homologous recombination [6,7]. Besides these methods which are based on the *in vitro* genetic engineering of pluripotent stem cells, transposon-mediated mutagenesis [8] and N-ethyl-N-nitrosourea (ENU) mutagenesis [9,10] have been used with some success for producing mutations in the rat genome. We recently reported on a high-throughput gene-driven strategy which uses the mutagen ENU and the Mu-transposition reaction (MuT-POWER) to rapidly detect induced mutations. This was in addition to our investigation of intracytoplasmic sperm injection (ICSI) for recovering heterozygous genotypes of interest out of a large sperm cell repository [11,12]. However, even if a large number of mutant strains already exists or may potentially be available, targeted modification or disruption of specific DNA regions is difficult to achieve. Even in the case of our gene-driven strategy, X-linked mutations are impossible to obtain because of the breeding protocol which is used [11].

Recently, a novel gene-targeting technology which employs zinc-finger nucleases (ZFNs) has been proven to work successfully in plants, *Caenorhabditis elegans*, frogs, drosophila, zebrafish, and human ESCs and iPSCs [13,14,15]. ZFNs are chimeric proteins that consist of a specific DNA-binding domain which is made of tandem zinc finger-binding motifs that are fused to a non-specific cleavage domain of the restriction endonuclease *Fok*I. ZFNs can create site-specific double-stranded breaks which are repaired via non-homologous end joining (NHEJ), a process that results in the arbitrary addition or deletion of base pairs. Consequently, repair by NHEJ is mutagenic and results in a knockout. Recently, it was reported that a single injection of DNA or messenger RNA that encodes specific ZFNs into one-cell transgenic rat embryos that express GFP could lead to a high frequency of animals that do not express the transgenic marker as a consequence of homologous recombination at the GFP site [16]. Here, we report on an experiment that involved using ZFN technology. The aim of the experiment was to inactivate the gene that encodes the interleukin 2 receptor gamma (*Il2rg*), which is essential for signaling by interleukins such as IL-2, IL-4, IL-7, IL-9, IL-15, and IL-21. In

addition, the gene is involved in the X-linked form of severe combined immunodeficiency (X-SCID), one of the most common forms of human SCID [17,18]. A major motivation for performing this experiment was the observation that although SCID mouse animal models are the most commonly used in research on drug development, an X-SCID immunodeficient rat model would complement mouse models through the additional advantage of being employed for testing the pharmacodynamics and toxicity of potential therapeutic compounds. Following the results of research involving *Prkdc* SCID [19,20] and *Il2rg* X-SCID mice [21,22,23], *Il2rg* X-SCID rats should have a very low level of NK cell activity and thereby make xenotransplantation more successful.

Results

Injection of *Il2rg* ZFN-encoding mRNA into rat embryos

Of 443 ZFN-injected embryos, 230 (51.9%) were transferred into the oviducts of pseudopregnant female rats, and 54 (24.3%) of these embryos were successfully carried to term as shown in Figure 1a, b and Table 1. Sequence analysis of the ZFN target site of these 54 founder animals revealed that 5 males and 8 females (24.1%) carried a variety of mutations including from 3 to1,097 bp deletions and a 1 bp insertion in the region which overlapped the ZFN target site as seen in Figure 1c and Figure S1. Four out of five of the males carried different biallelic mutations at the *Il2rg* locus despite them only having one X chromosome. This suggests that mosaicism was induced by the ZFN treatment, a situation which is frequently observed in the DNA of transgenic founders. Three of the affected females had a monoallelic homozygous mutation, four had heterologous or mosaicism biallelic mutations, and the remainder had three different mosaic mutations. The normal F344-allele was not found in the affected founder animals. Most of these mutations were expressed as frameshifts or splicing errors and resulted in no or very little IL2RG mRNA being expressed as shown in Figure 1d probably due to nonsense-mediated decay. Western blotting with antibodies against the C-terminal domain of

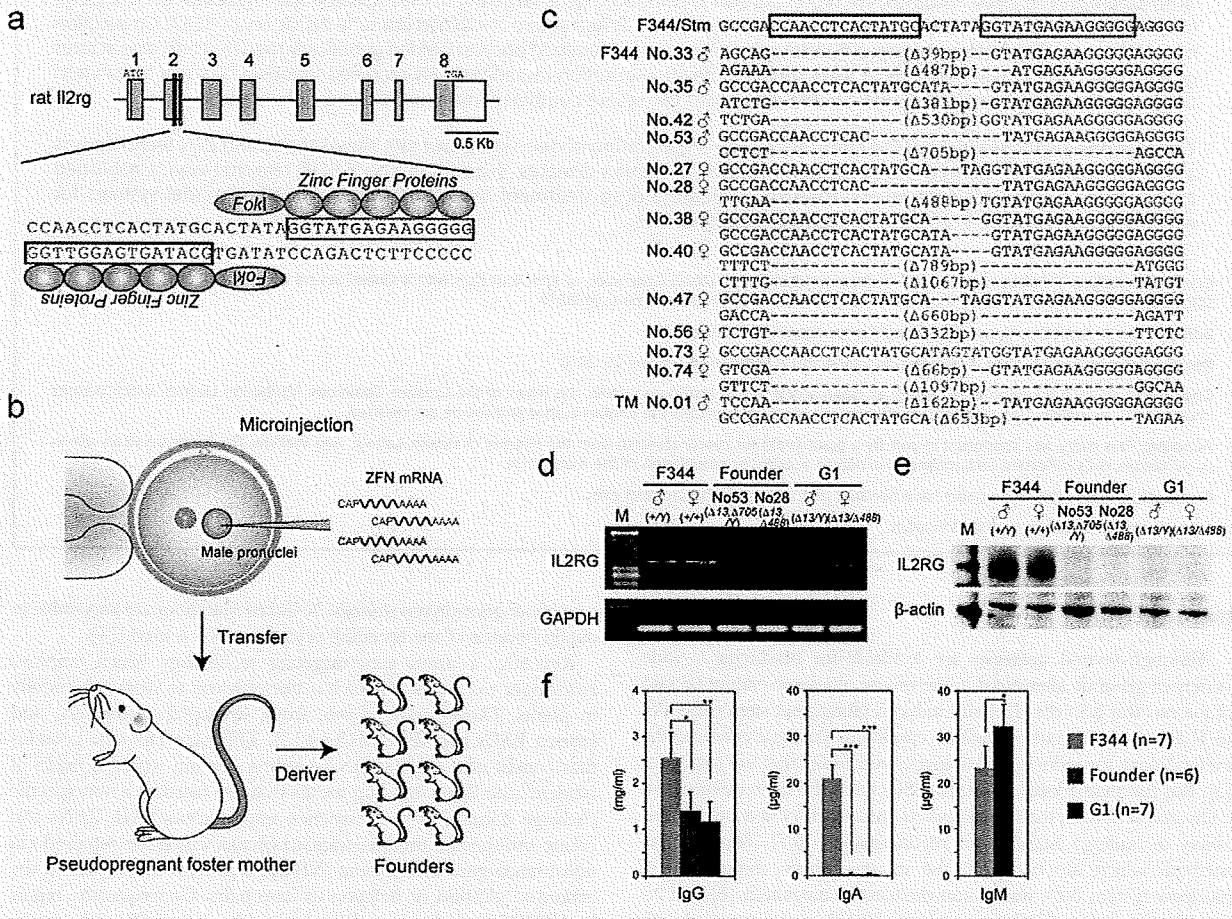

Figure 1 Injection of *Il2rg* ZFN-encoding mRNA into rat embryos induced targeted loss-of-function mutations. (a) Schematic representation of the rat *Il2rg* gene. Exons are represented as blue boxes. Regions used to design the ZFN templates are printed in red for the left ZFN and green for the right ZFN. The magnified views illustrate the binding sites for the ZFN pairs. Please see Figure S4 for further details. (b) Schematic representation of the method used for ZFN-targeted mutagenesis in rat embryos. (c) Sequencing assay for ZFN-induced mutations in the *Il2rg*-targeted region. Multiple deletions or insertions depicted using red dashes or letters, respectively, are aligned along the wild-type sequences shown on the top line. (d) RT-PCR analysis of IL2RG mRNA expression in the spleen of control F344, founder (G0), and G1 rats. GAPDH expression was used as an internal control. (e) Western blotting for IL2RG protein in the spleen of control F344, founder (G0), and G1 rats. β-actin was used as a loading control. (f) ELISA for serum IgG, IgA, and IgM levels in control F344, founder (G0), and G1 rats. *P<0.01, **P<0.001, and ***P<0.0001, indicated for each group in comparison with control F344 for independent sample Student t-tests.
doi:10.1371/journal.pone.0008870.g001

Table 1. Injection of ZFN-encoding mRNA into fertilized oocytes.

Strain	Oocyte state	Injected oocytes	Transferred oocytes (%)	Born (%)	Mutants (%)
F344/Stm	Fresh	234	32 (-)	♂2,♀5 (21.9)	♀2 (28.6)
	Cryopreserved[a]		57 (-)	♂8,♀10 (31.6)	♀2 (11.1)
	Fresh	182	129 (68.3)	♂16,♀11 (20.9)	♂4,♀4 (29.6)
TM/Kyo	Fresh	27	12 (44.4)	♂1,♀1 (16.7)	♂1 (50.0)
Total		**443**	**230 (51.9)**	**♂27,♀27 (24.3)**	**♂5,♀8 (24.1)**

[a]Injected oocytes were cultured in KRB overnight and cryopreserved at the two-cell stage.
doi:10.1371/journal.pone.0008870.t001

IL2RG did not reveal any protein in the founder animals as seen in Figure 1e.

To clarify whether the ZFNs only induced mutations in the targeted region, we checked 16 sites that showed a high rate of similarity with the targeted site at the sequence level with no more than 6 to 7 bp mismatches as illustrated in Table S1. Insertions or deletions were not observed at any of these off-target sites among the 13 ZFN-modified founders. This confirms that ZFNs can be reliably and efficiently used to produce mutant alleles at loci of interest. Although we cannot exclude the possibility that the ZFNs may have cleaved unknown off-target sites, such undesired mutations can subsequently be easily excluded from the genome of the carrier animals by backcrossing to the parental strain or another background strain.

Germ line transmission of ZFN-modified genetic changes

To assess the transmission of ZFN-modified genetic changes to the next generation, we crossed the founder animals with the background strain F344/Stm as depicted in Table S2. All 38 offspring consisting of 18 males and 20 females that were obtained from the founder females mated with the F344 males had one of the maternal mutations. This indicates that ZFN-induced mutations were faithfully transmitted through the germ line. In the offspring that were obtained from the founder males, there were two cases where only one of the paternal bialleles was transmitted or both alleles were transmitted. This suggests that mosaicism occurred not only in somatic cells but also in the germ line of the founder animals. PCR analysis of genomic DNA isolated from several types of tissues indicated that somatic mosaicism occurred in the progenitors but not in their offspring as shown in Figure S2.

We intercrossed the G0 founders to produce hemizygous males (*Il2rg*$^{-}$/*Y*) and homozygous females (*Il2rg*$^{-}$/*Il2rg*$^{-}$) for the ZFN-induced mutation listed in Table S3 to characterize the immunodeficient phenotypes of the X-SCID rats. The hemizygous males and homozygous females appeared normal at birth and developed well as shown in Figure 2a. RT-PCR and Western blot assays was performed on these G1 rats and the results showed a complete loss of expression of the *Il2rg* gene as detailed in Figures 1d, e. ELISA for serum immunoglobulin (Ig) levels revealed reduced IgG, diminished IgA, and increased IgM levels in the G1 rats as noted in Figure 1f.

Characterization of *Il2rg*-deficient X-SCID rats

Gross and microscopic analyses at five weeks of age showed that the X-SCID rats underwent abnormal lymphoid development as depicted in Figure 2. The thymus of X-SCID rats was extremely hypoplastic as seen in Figure 2b and consisted of an epithelial rudiment without any lymphocytes as seen in Figure 2d. The spleen was moderately decreased in size as noted in Figure 2c, and the white pulp was severely hypoplastic and the red pulp contained myeloid cells as shown in Figure 2f. Peripheral lymph nodes and Peyer's patches were not identified by necropscopy. In the peripheral blood (PB) profiles, the numbers of white blood cells (WBCs) was reduced compared to those of control rats as detailed in Table S4. Differential counts of WBCs showed a dramatic decrease in leukocytes in the X-SCID rats (Table S5). Flow cytometry analysis of cell populations isolated from PB, bone marrow (BM), and the spleen also revealed a dramatic decrease in the number of the lymphocytes as seen in Figure 2h and Figure S3. The number of $CD4^{-}CD8^{+}$ T-cells was markedly diminished and the number of $CD4^{+}CD8^{-}$ T-cells was decreased although some cells were present in PB, BM and the spleen. The numbers of $CD3^{-}CD45RA^{+}$ B-cells and $CD3^{-}CD161a^{+}$ NK cells were markedly diminished in PB and BM, but some cells were present in the spleen. Heterozygous females exhibited normal lymphoid development and were indistinguishable from normal control females (data not shown).

Xenotransplantation of human tumor cells

These immunodeficient phenotypes of the X-SCID rats were very similar to those of the previously reported X-SCID mice and were characterized by a nearly complete lack of T-cells, B-cells and NK cells [21,22,23]. Since X-SCID mice cannot reject transplanted tissues from other species including humans, we tested *Il2rg*-deficient rats as a host for xenotransplantation of human ovarian cancer tumor cells. All X-SCID rats developed tumors within 14 days after injection of the cells (6/6, 100%), while control F344 rats showed no tumor growth (0/6, 0%) as seen in Figure 3a, b. The tumors were confirmed by histological analysis as depicted in Figure 3c and by PCR with primers that were used to amplify the human MHC class II DQB2 region (data not shown). These observations illustrate the impaired immune system function of X-SCID rats and suggest that the animals may be important models for cancer and transplantation research.

Discussion

In this study, we proved that targeted gene disruption using ZFN technology works well and provides for several advantages and possibilities when used in rats. First and foremost, knockout rats can be created in a four- to six-month time frame and with high efficiency at more than 20%. This is more favorable than the ES cell-based method for mice that usually takes 12–18 months. Given the high rate of germ line transmission, preliminary phenotypic analysis can be performed on G1 animals after intercrossing the initial G0 founders, thereby saving time and effort. Second, gene-targeting with ZFNs does not seem to be strain-dependent (unpublished data) and accordingly can be performed with any inbred strain. This is of great advantage

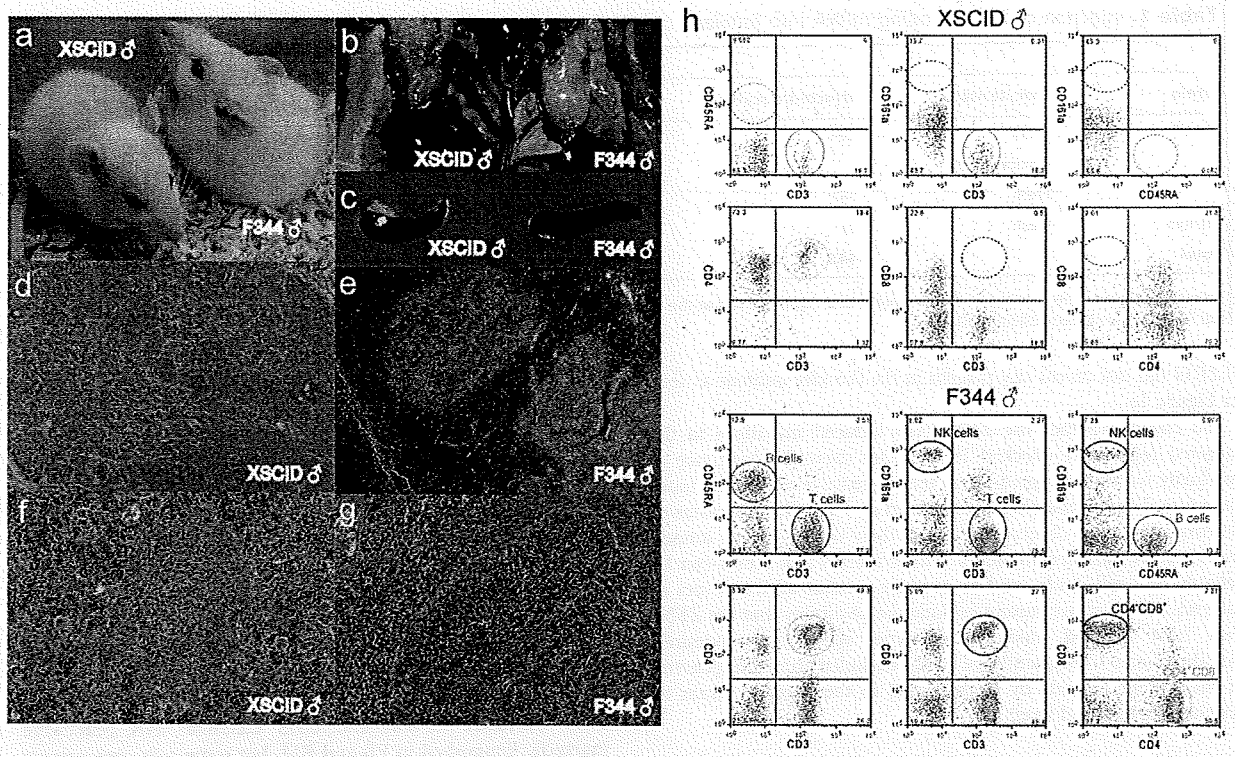

Figure 2 Abnormal lymphoid development in X-SCID rats. (a) Photograph of five week-old male X-SCID (*Il2rg*$^{-}$/*Y*) and F344 (+/*Y*) rats. (b) Thymus of X-SCID and F344 rats. (c) Spleen of X-SCID and F344 rats. (d, e) Histological analysis of the thymus of X-SCID (X40) and F344 (X40) rats. The thymus of the X-SCID rat was severely hypoplastic and consisted of an epithelial cell sheet. (f, g) Histological analysis of the spleen of X-SCID (X100) and F344 (X100) rats. In the X-SCID spleen, the white pulp was virtually devoid of lymphocytes and the red pulp was occupied by a variety of myeloid elements. (h) Dot plots representing CD3, CD45RA and CD161a for differentiation of T-, B- and NK cell sub-populations, and CD3, CD4 and CD8 for demarcation of T-cell sub-populations in peripheral blood lymphocyte cells. The numbers shown in the quadrants are mean percentages. The circled areas indicate cell populations that are referred to in the text.
doi:10.1371/journal.pone.0008870.g002

since other techniques like ENU mutagenesis differ in their efficiency when used with different strains. This provides a straight forward strategy for directly employing targeted gene disruption in the existing strain, thereby bypassing tedious and time-consuming backcrossing steps that generally take two to three years to complete. Third, ZFNs can be used to induce a wide variety of allelic changes covering small or wide deletions or insertions. They may be used to produce frameshifts or small in-frame deletions such as the 3-bp deletion that we observed. Given the reports on successful ZFN-targeted gene modification or correction by homologous recombination in mammalian cell cultures [15,24,25], it should be feasible to archive targeted knock-in technologies that have thus been far inaccessible without rat ES cells. Finally, since ZFN technology does not rely on using species-specific embryonic stem cell lines, it should be possible to adapt it to other mammalian species such as pigs, cattle, and monkeys, where it is possible to harvest and manipulate fertilized embryos.

The X-SCID rats established in this study provide not only a valuable *in vivo* model for evaluating drug treatment or gene therapy approaches, but also a system for assaying novel anticarcinogenic effects on transplanted malignancies. There is a growing need for animal models with which to carry out *in vivo* studies using human cells, tissues or organs as chimeras such as humanized models [26,27,28]. X-SCID and SCID mice homozygous for *Il2rg*- and *Prkdc*- alleles with a non-obese diabetic background are a powerful tool for the xenotransplantation of human tissues or potentially human ES/iPS cells. This could lead to advances in our understanding of human hematopoiesis, immunology, cancer biology, infectious diseases, and regenerative medicine [29,30,31]. Humanized rats, if generated by ZFN technology, could be powerful tools for pre-clinical testing during drug development and be better models in various fields of translational research.

Materials and Methods

Animals

All animal care and experiments conformed to the Guidelines for Animal Experiments of Kyoto University, and were approved by the Animal Research Committee of Kyoto University. F344-*Il2rg*^{tm1Kyo} X-SCID rats are deposited at the National Bio Resource Project for the Rat in Japan (www.anim.med.kyoto-u.ac.jp/nbr).

ZFN constructs

Custom-designed ZFNs plasmids for the rat *Il2rg* gene were obtained from Sigma-Aldrich. The design, cloning, and validation of the ZFNs was performed by Sigma-Aldrich [32]. ZFN design involved using an archive of pre-validated two-finger and one-finger modules [32,33]. The target region was scanned for positions where modules exist in the archive. This allowed the fusion of two or three such molecules to generate a five-finger

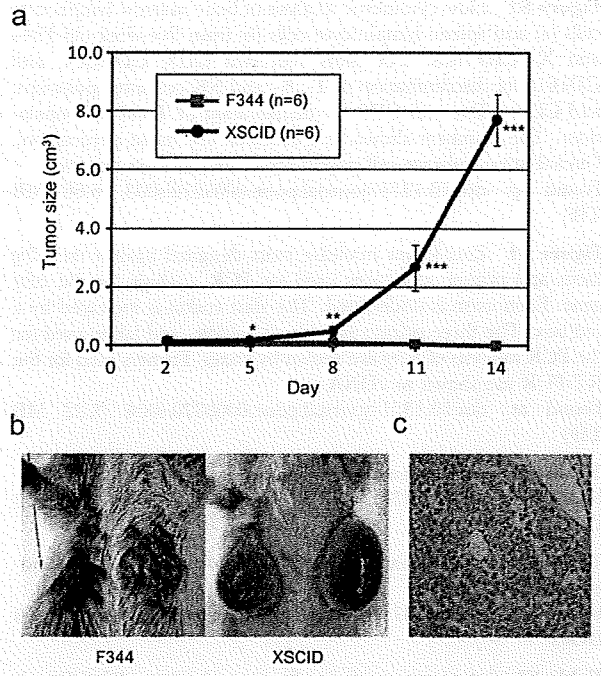

Figure 3 Tumor development from the xenotransplantation of human ovarian cancer cells. (a) Growth curve of tumor development after subcutaneous injection of A2780 human ovarian cancer cells in F344 and X-SCID rats. *P<0.01, **P<0.001, and ***P<0.0001, indicated in comparison with control F344. (b) The tumors became large and grew quickly about 11 days after injection in X-SCID rats but not in F344 rats. (c) Histology of the xenotransplanted tumors that formed in X-SCID rats (X400). No lymphocytic infiltration was detected in the tumors.
doi:10.1371/journal.pone.0008870.g003

protein that recognizes a 15 bp site on the top strand and the fusion of two to three different modules that recognize a 15 bp site on the bottom strand that lies 5–6 bp away. Measurements of ZFNs for gene disruption activity were performed using the Surveyor endonuclease (CEL-1) assay as described elsewhere [34]. Final candidate ZFNs were designed to recognize a site within the boundary between exon 2 and intron 2 of the *Il2rg* gene as shown in Figure S4.

Microinjection of ZFN mRNA

To prepare ZFN mRNA, ZFN-encoding expression plasmids were linearized with *Xho*I and extracted with phenol-chloroform by the standard method. Messenger RNA was transcribed *in vitro* using a MessageMax^{TM} T7 mRNA transcription kit (Epicentre) and polyadenylated using a A-Plus^{TM} Poly(A) polymerase tailing kit (Epicentre). The resulting mRNA was purified using a MEGAClear^{TM} kit (Epicentre) and finally resuspended in RNase-free water at 10 ng/μl for each ZFN. Approximately 2–3 pL of capped mRNA were injected into the male pronuclei of zygotes by the same method that was used to microinject DNA. Pronuclear stage embryos were collected from F344/Stm and TM/Kyo females six weeks of age that had been super-ovulated by injecting them with eCG (Serotropin, Asuka Pharmaceutical Co.) and hCG (Gonatropin, Asuka Pharmaceutical Co.). They were mated with males of the same respective strain. The mRNA solution was injected and embryos were cultured in KRB at 37.5°C with 5% CO_2 and 95% humidified air to promote their recovery. The embryos that survived were transferred to the oviduct of pseudopregnant females (Crlj:WI, 8–12wks).

Analysis of genome editing at ZFN target sites

Genomic DNA was extracted from the tail, brain, heart, and liver using a GENEXTRACTOR TA-100 automatic DNA purification system (Takara). PCR for each was carried out in a total volume of 15 μl under the following conditions for 35 cycles: 94°C for 3 min for 1 cycle, 94°C for 30 sec, 60°C for 30 sec, and 72°C for 1 min. The final reaction mixture for each contained 100 ng of genomic DNA, 200 μM of each dNTP, 1.0 mM $MgCl_2$, 0.66 μM of each primer, and 0.4 U of Taq DNA polymerase (GibcoBRL).

For editing the ZFN cleavage site in the genome at the *Il2rg* locus, three primer sets were designed to amplify small 292-bp, middle 1509-bp, and large 3158-bp fragments as shown in Figure S4. The PCR products were directly sequenced using the BigDye terminator v3.1 cycle sequencing mix and the standard protocol for an Applied Biosystems 3130 DNA Sequencer. The products were also subcloned into the pCR4-TOPO vector (Invitrogen), and plasmid DNA was prepared and sequenced on a 3130 DNA Sequencer. All new sequence data is deposited in GenBank (GU294902-GU294925).

Off-target site analysis

Off-target sites with the highest degree of similarity were identified by searching the rat genome (RGSCv3.4) for matches with the consensus sequence of each ZFP with appropriate spacing of 5–6 bp. A list of these target sites is provided in Supplementary Table 1. PCR primers were designed to flank the off-target sites as detailed in Table S6. Reactions were performed for the founder animals and the PCR products were directly sequenced on the 3130 DNA Sequencer.

RT-PCR and Western blotting

Total RNA was extracted using Isogen reagent (Nippon Gene) from the spleen of five week-old rats. First strand cDNA was synthesized from 5 μg of total RNA that had been treated using DNase by using the oligo(dT)12–18 primer and SuperscriptII reverse transcriptase (Invitrogen). PCR was performed with the primers for *Il2rg* described in Figure S4 and with the *Gapdh* 5′-GGCACAGTCAAGGCTGAGAATG-3′ and 5′-ATGGTGGT-GAAGACGCCAGTA-3′. Western blotting was carried out using the cell lysates from the spleens of five week-old rats by the standard method. Signals were detected with antibodies against rat IL2RG (M-20, Santa Cruz Biotechnology) and β-actin (AC-40, Sigma Aldrich).

Immunofluorescence and histological analyses

Complete necroscopy examinations were performed on five week-old *Il2rg*-deficient and wild-type male and female rats. Peripheral blood specimens were collected from the caudal vena cava. Serum immunoglobulin (Ig) levels were measured by enzyme-linked immunosorbent assay (ELISA) using Rat IgG, IgA and IgM ELISA Quantitation kits (Bethyl Laboratories). Blood parameters for a complete blood cell count, a WBC differential, and a reticulocyte count were measured using ADVIA 2120 flow cytometry (Block Scientific). For histopathology, tissues were fixed in Bouin's fluid and embedded in paraffin. The embedded tissues were then sectioned at 5–7 μm thickness at room temperature and stained with hematoxylin and eosin to permit evaluation by light microscopy.

Flow cytometric analyses of cell populations isolated from bone marrow, the spleen and peripheral blood were carried out using IOTest Anti-Rat CD3-FITC/CD45RA-PC7/CD161a-APC (Beckman Coulter) to differentiate T-, B- and NKcell sub-populations and IOTest Anti-Rat CD3-FITC/CD4-PC7/CD8-APC (Beckman Coulter) to enumerate T-cell sub-populations. Anti-CD45 monoclonal antibodies (Beckman Coulter) were used for the intracellular staining of lymphocytes. Mouse IgM, IgG1 and IgG2a antibodies (Beckman Coulter) were used as isotype-matched controls. The cell samples were treated with FcR-blocking reagent (Miltenyi Biotec) for 10 minutes, stained with the fluorochrome-conjugated antibodies for 30 minutes, and washed three times with PBS/10% FCS. Stained cell samples were analyzed with a four-color FACS flow cytometer (FACSCalibur, Becton Dickinson) using CellQuest software (Becton Dickinson).

Tumor cell xenotransplantation

The human ovarian cancer cell line A2780 was purchased from the European Collection of Cell Cultures (ECACC). Cells were cultured in RPMI1640 medium (GIBCO) with 10% heat-inactivated FBS (Hyclone). Subcutaneous injections of 2×10^5 A2780 cells with Matrigel (Becton Dickinson) were performed on five week-old female rats. Tumors were measured by length (a) and width (b) in millimeters using calipers, and tumor volumes (V) were calculated according to the relationship $V=ab^2/2$, where a was the longer of the two measurements. Human-specific PCR primers were designed to amplify major histocompatibility complex class II DQ beta 2 (HLA-DQB2) at exon 4 as follows: 5′-CCTAGG-GTGGTCAGACTGGA-3′ and 5′-AAAATCCCCCAAAACA-AAGG-3′.

Supporting Information

Figure S1 PCR analysis of 13 mutant founders for the zinc-finger nuclease (ZFN) target site. For the analysis of the ZFN target site at the *Il2rg* locus, three primer sets were used to amplify small (a, 292-bp), middle (b, 1509-bp), and large (c, 3158-bp) fragments for PCR. See Figure S4 for further details. PCR fragments were electrophoresed through a 1-4% agarose gel. M: DNA molecular weight marker ϕX174-*Hae*III digest.
Found at: doi:10.1371/journal.pone.0008870.s001 (9.19 MB TIF)

Figure S2 PCR analysis of genomic DNA isolated from several tissues. Three primer sets were used to amplify small (a, 292-bp), middle (b, 1509-bp), and large (c, 3158-bp) fragments for PCR. See Figure S4 for further details. Genomic DNA (T: tail, B: brain, H: heart, L: liver) was used as a template for PCR in zinc-finger nuclease-modified founders (numbers 28, 35, 40, and 53) and G1 rats. PCR fragments were electrophoresed through a 1–4% agarose gel. M: DNA molecular weight marker ϕX174-*Hae*III digest or Lambda DNA-*Hind*III digest.
Found at: doi:10.1371/journal.pone.0008870.s002 (6.28 MB TIF)

Figure S3 Flow cytometric analysis of bone marrow lymphocyte cells (a) and spleen lymphocyte cells (b) from five-week-old F344 and X-SCID rats. Dot plots represent CD3, CD45RA, and CD161a for discrimination of T-, B-, and NK cell subpopulations; and CD3, CD4, and CD8 for demarcation of T cell subpopulations. The numbers shown in quadrants are mean percentages. Circled areas indicate cell populations referred to in the text.
Found at: doi:10.1371/journal.pone.0008870.s003 (6.66 MB TIF)

Figure S4 Zinc-finger nuclease pairs designed against the *Il2rg* locus and primer sequences used for PCR analysis for the *Il2rg* gene. Each exon is underlined. The start codon is indicated by a red box. The three primer sets (small, middle, and large) used for the PCR analysis of *Il2rg* are shown by boxes. Primers used for the RT-PCR are shown as cDNA.
Found at: doi:10.1371/journal.pone.0008870.s004 (3.32 MB TIF)

Table S1 Potential zinc-finger nuclease off-target sites.
Found at: doi:10.1371/journal.pone.0008870.s005 (0.14 MB DOC)

Table S2 Backcrossing of zinc-finger nuclease-modified founders to F344/Stm rats.
Found at: doi:10.1371/journal.pone.0008870.s006 (0.16 MB DOC)

Table S3 Intercrossing of zinc-finger nuclease-modified founders between males and females.
Found at: doi:10.1371/journal.pone.0008870.s007 (0.08 MB DOC)

Table S4 Peripheral blood profiles of *Il2rg*-deficient (X-SCID) rats.
Found at: doi:10.1371/journal.pone.0008870.s008 (0.09 MB DOC)

Table S5 Differential counts of the white blood cells of *Il2rg*-deficient (X-SCID) rats.
Found at: doi:10.1371/journal.pone.0008870.s009 (0.07 MB DOC)

Table S6 Primer sequences for zinc-finger nuclease off-target analysis.
Found at: doi:10.1371/journal.pone.0008870.s010 (0.14 MB DOC)

Acknowledgments

This study was supported in part by a Grant-in-aid for Cancer Research from the Ministry of Health, Labour and Welfare. We thank JL Guénet for critical discussion, and Y Kunihiro, F Tagami, and S Ishida for their assistance with the experiment.

Author Contributions

Conceived and designed the experiments: TM BV TS. Performed the experiments: TM AT KY HH TK. Analyzed the data: TM. Wrote the paper: TM.

References

1. Li P, Tong C, Mehrian-Shai R, Jia L, Wu N, et al. (2008) Germline competent embryonic stem cells derived from rat blastocysts. Cell 135: 1299–1310.
2. Buehr M, Meek S, Blair K, Yang J, Ure J, et al. (2008) Capture of authentic embryonic stem cells from rat blastocysts. Cell 135: 1287–1298.
3. Liao J, Cui C, Chen S, Ren J, Chen J, et al. (2009) Generation of induced pluripotent stem cell lines from adult rat cells. Cell Stem Cell 4: 11–15.
4. Li W, Wei W, Zhu S, Zhu J, Shi Y, et al. (2009) Generation of rat and human induced pluripotent stem cells by combining genetic reprogramming and chemical inhibitors. Cell Stem Cell 4: 16–19.
5. Voigt B, Serikawa T (2009) Pluripotent stem cells and other technologies will eventually open the door for straightforward gene targeting in the rat. Dis Model Mech 2: 341–343.
6. Ryu BY, Kubota H, Avarbock MR, Brinster RL (2005) Conservation of spermatogonial stem cell self-renewal signaling between mouse and rat. Proc Natl Acad Sci U S A 102: 14302–14307.
7. Shinohara T, Kato M, Takehashi M, Lee J, Chuma S, et al. (2006) Rats produced by interspecies spermatogonial transplantation in mice and in vitro microinsemination. Proc Natl Acad Sci U S A 103: 13624–13628.

8. Kitada K, Ishishita S, Tosaka K, Takahashi R, Ueda M, et al. (2007) Transposon-tagged mutagenesis in the rat. Nat Methods 4: 131–133.
9. Zan Y, Haag JD, Chen KS, Shepel LA, Wigington D, et al. (2003) Production of knockout rats using ENU mutagenesis and a yeast-based screening assay. Nat Biotechnol 21: 645–651.
10. Smits BM, Mudde JB, van de Belt J, Verheul M, Olivier J, et al. (2006) Generation of gene knockouts and mutant models in the laboratory rat by ENU-driven target-selected mutagenesis. Pharmacogenet Genomics 16: 159–169.
11. Mashimo T, Yanagihara K, Tokuda S, Voigt B, Takizawa A, et al. (2008) An ENU-induced mutant archive for gene targeting in rats. Nat Genet 40: 514–515.
12. Yoshimi K, Tanaka T, Takizawa A, Kato M, Hirabayashi M, et al. (2009) Enhanced colitis-associated colon carcinogenesis in a novel Apc mutant rat. Cancer Sci.
13. Porteus MH, Carroll D (2005) Gene targeting using zinc finger nucleases. Nat Biotechnol 23: 967–973.
14. Wu J, Kandavelou K, Chandrasegaran S (2007) Custom-designed zinc finger nucleases: what is next? Cell Mol Life Sci 64: 2933–2944.
15. Hockemeyer D, Soldner F, Beard C, Gao Q, Mitalipova M, et al. (2009) Efficient targeting of expressed and silent genes in human ESCs and iPSCs using zinc-finger nucleases. Nat Biotechnol 27: 851–857.
16. Geurts AM, Cost GJ, Freyvert Y, Zeitler B, Miller JC, et al. (2009) Knockout rats via embryo microinjection of zinc-finger nucleases. Science 325: 433.
17. Noguchi M, Yi H, Rosenblatt HM, Filipovich AH, Adelstein S, et al. (1993) Interleukin-2 receptor gamma chain mutation results in X-linked severe combined immunodeficiency in humans. Cell 73: 147–157.
18. Leonard WJ (2001) Cytokines and immunodeficiency diseases. Nat Rev Immunol 1: 200–208.
19. Blunt T, Finnie NJ, Taccioli GE, Smith GC, Demengeot J, et al. (1995) Defective DNA-dependent protein kinase activity is linked to V(D)J recombination and DNA repair defects associated with the murine scid mutation. Cell 80: 813–823.
20. Kirchgessner CU, Patil CK, Evans JW, Cuomo CA, Fried LM, et al. (1995) DNA-dependent kinase (p350) as a candidate gene for the murine SCID defect. Science 267: 1178–1183.
21. Cao X, Shores EW, Hu-Li J, Anver MR, Kelsall BL, et al. (1995) Defective lymphoid development in mice lacking expression of the common cytokine receptor gamma chain. Immunity 2: 223–238.
22. DiSanto JP, Muller W, Guy-Grand D, Fischer A, Rajewsky K (1995) Lymphoid development in mice with a targeted deletion of the interleukin 2 receptor gamma chain. Proc Natl Acad Sci U S A 92: 377–381.
23. Ohbo K, Suda T, Hashiyama M, Mantani A, Ikebe M, et al. (1996) Modulation of hematopoiesis in mice with a truncated mutant of the interleukin-2 receptor gamma chain. Blood 87: 956–967.
24. Urnov FD, Miller JC, Lee YL, Beausejour CM, Rock JM, et al. (2005) Highly efficient endogenous human gene correction using designed zinc-finger nucleases. Nature 435: 646–651.
25. Kandavelou K, Ramalingam S, London V, Mani M, Wu J, et al. (2009) Targeted manipulation of mammalian genomes using designed zinc finger nucleases. Biochem Biophys Res Commun 388: 56–61.
26. Dao MA, Tsark E, Nolta JA (1999) Animal xenograft models for evaluation of gene transfer into human hematopoietic stem cells. Curr Opin Mol Ther 1: 553–557.
27. Thomsen M, Yacoub-Youssef H, Marcheix B (2005) Reconstitution of a human immune system in immunodeficient mice: models of human alloreaction in vivo. Tissue Antigens 66: 73–82.
28. Shultz LD, Ishikawa F, Greiner DL (2007) Humanized mice in translational biomedical research. Nat Rev Immunol 7: 118–130.
29. Ito M, Kobayashi K, Nakahata T (2008) NOD/Shi-scid IL2rgamma(null) (NOG) mice more appropriate for humanized mouse models. Curr Top Microbiol Immunol 324: 53–76.
30. Quintana E, Shackleton M, Sabel MS, Fullen DR, Johnson TM, et al. (2008) Efficient tumour formation by single human melanoma cells. Nature 456: 593–598.
31. Machida K, Suemizu H, Kawai K, Ishikawa T, Sawada R, et al. (2009) Higher susceptibility of NOG mice to xenotransplanted tumors. J Toxicol Sci 34: 123–127.
32. Doyon Y, McCammon JM, Miller JC, Faraji F, Ngo C, et al. (2008) Heritable targeted gene disruption in zebrafish using designed zinc-finger nucleases. Nat Biotechnol 26: 702–708.
33. Santiago Y, Chan E, Liu PQ, Orlando S, Zhang L, et al. (2008) Targeted gene knockout in mammalian cells by using engineered zinc-finger nucleases. Proc Natl Acad Sci U S A 105: 5809–5814.
34. Miller JC, Holmes MC, Wang J, Guschin DY, Lee YL, et al. (2007) An improved zinc-finger nuclease architecture for highly specific genome editing. Nat Biotechnol 25: 778–785.

Involvement of JNK pathway in the promotion of the early stage of colorectal carcinogenesis under high-fat dietary conditions

H Endo, K Hosono, T Fujisawa, et al.

Gut 2009 58: 1637-1643 originally published online June 30, 2009
doi: 10.1136/gut.2009.183624

Involvement of JNK pathway in the promotion of the early stage of colorectal carcinogenesis under high-fat dietary conditions

H Endo,[1] K Hosono,[1] T Fujisawa,[1] H Takahashi,[1] M Sugiyama,[1] K Yoneda,[1] Y Nozaki,[1] K Fujita,[1] M Yoneda,[1] M Inamori,[1] K Wada,[2] H Nakagama,[3] A Nakajima[1]

See Commentary, p 1575

► Supplementary material (a method and four figures) is published online only at http://gut.bmj.com/content/vol58/issue12

[1] Division of Gastroenterology, Yokohama City University School of Medicine, Yokohama, Japan; [2] Department of Pharmacology, Graduate School of Dentistry, Osaka University, Osaka, Japan; [3] Biochemistry Division, National Cancer Center Research Institute, Tokyo, Japan

Correspondence to: Dr A Nakajima, 3-9 Fuku-ura, Kanazawa-ku, Yokohama 236-0004, Japan; nakajima-tky@umin.ac.jp

Revised 27 May 2009
Accepted 10 June 2009
Published Online First 30 June 2009

ABSTRACT

Background and aims: The molecular mechanisms underlying the promotion of colorectal carcinogenesis by a high-fat diet (HFD) remain unclear. We investigated the role of the insulin-signal pathway and the c-Jun N-terminal kinase (JNK) pathway, which reportedly play crucial roles in insulin resistance, during colorectal carcinogenesis in the presence of hyperinsulinaemia induced by a HFD.

Methods: Azoxymethane-induced aberrant crypt foci formation and cell proliferation in the colonic epithelium were compared between mice fed a normal diet (ND) and mice fed a HFD. A western blot analysis was performed to elucidate the mechanism affecting colorectal carcinogenesis by a HFD.

Results: The number of aberrant crypt foci and the colonic epithelial cell proliferative activity were significantly higher in the HFD group than in the ND group. While the plasma insulin level was significantly higher in the HFD group than in the ND group, a western blot analysis revealed the inactivation of Akt, which is located downstream of the insulin receptor, in the colonic epithelia of the HFD group. On the other hand, JNK activity was significantly higher in the HFD group than in the ND group. A JNK specific inhibitor significantly suppressed the increase in epithelial cell proliferation only under a HFD, but not under a ND.

Conclusions: Colonic cell proliferation was promoted via the JNK pathway in the presence of a HFD but not in the presence of a ND. This novel mechanism may explain the involvement of the JNK pathway in the effect of dietary fat intake on colon carcinogenesis.

Colorectal cancer is a major cause of morbidity and mortality worldwide.[1] Recently, associations between obesity and metabolic abnormalities, which are caused by a high intake of dietary fat and physical inactivity, and an elevated risk of colorectal cancer have been reported.[2 3] Many epidemiological studies have provided evidence of a relation between dietary fat intake and an increased risk of colorectal cancer.[4] Most animal experimental studies have shown that a high-fat diet (HFD) leads to an increased number of chemically induced aberrant crypt foci (ACF),[5] which are identifiable lesions in experimental colon carcinogenesis, and tumours[6] in the colon. The possibility that an elevated plasma insulin level promotes colorectal cancer has also been debated.[7] Some studies support the hypothesis that insulin, when exogenously administered, acts as an important growth factor for colonic epithelial cells.[8 9] However, whether an elevated plasma insulin level might enhance the proliferative state through the activation of an insulin signalling pathway downstream of the insulin receptor, such as the phosphatidylinositol 3-kinase (PI3K)/Akt signalling pathway, in the colon – a non-classical insulin target tissue – remains unclear.[10] Furthermore, adipocytokines also act as positive or negative modulators of colonic epithelium and tumours.[11 12] We previously reported that adiponectin suppressed colorectal carcinogenesis only under a HFD condition.[12] Despite accumulating evidence, the molecular mechanisms underlying the influence of a high intake of dietary fat on the promotion of colorectal carcinogenesis are not fully understood. The identification and evaluation of the relation between colorectal cancer and a high intake of dietary fat will be critical for preventive strategies against colorectal cancer in the near future.

Recent studies have demonstrated that c-Jun N-terminal kinase (JNK) plays a crucial role in obesity and insulin resistance.[13] JNK is activated in obesity, in part because of lipotoxic stress.[14] Hirosumi *et al*[13] reported abnormally elevated JNK activity levels in the liver, muscle and adipose tissues of mice fed a HFD. Most of the molecular mechanisms of JNK activity and their relation to insulin resistance have been studied in the liver and adipose tissues of various models of obesity, but little is known about the action of JNK in colonic epithelial cells. We postulated that JNK might provide a link between dietary fat intake and colorectal cancer.

The JNK pathway represents one subgroup of mitogen-activated protein kinases (MAPK) that is activated primarily by cytokines and exposure to environmental stress.[15] A major target of the JNK signalling pathway is the activator protein-1 (AP-1) transcription factor, which is activated, in part, by the phosphorylation of c-Jun and related molecules.[16] JNK has been implicated in the pathogenesis of cancer in various tissues in oncogenic transformation and cell proliferation.[15] Genetic and pharmacological approaches have been used to evaluate the potential importance of JNK in tumour formation and growth.[17 18] Growth inhibition has been observed in response to the JNK inhibitor and antisense oligonucleotides in multiple myeloma cells[19] and breast cancer cells.[20] Nateri *et al*[21] used a mouse model of intestinal tumorigenesis to show that the ablation of the c-Jun gene or the mutation of the JNK phosphorylation sites on c-Jun reduced the tumour number and size. These oncogenic functions of c-Jun are dependent on the N-terminal phosphorylation of c-Jun by JNK, implicating JNK as a potential oncogene in the intestine. Several studies

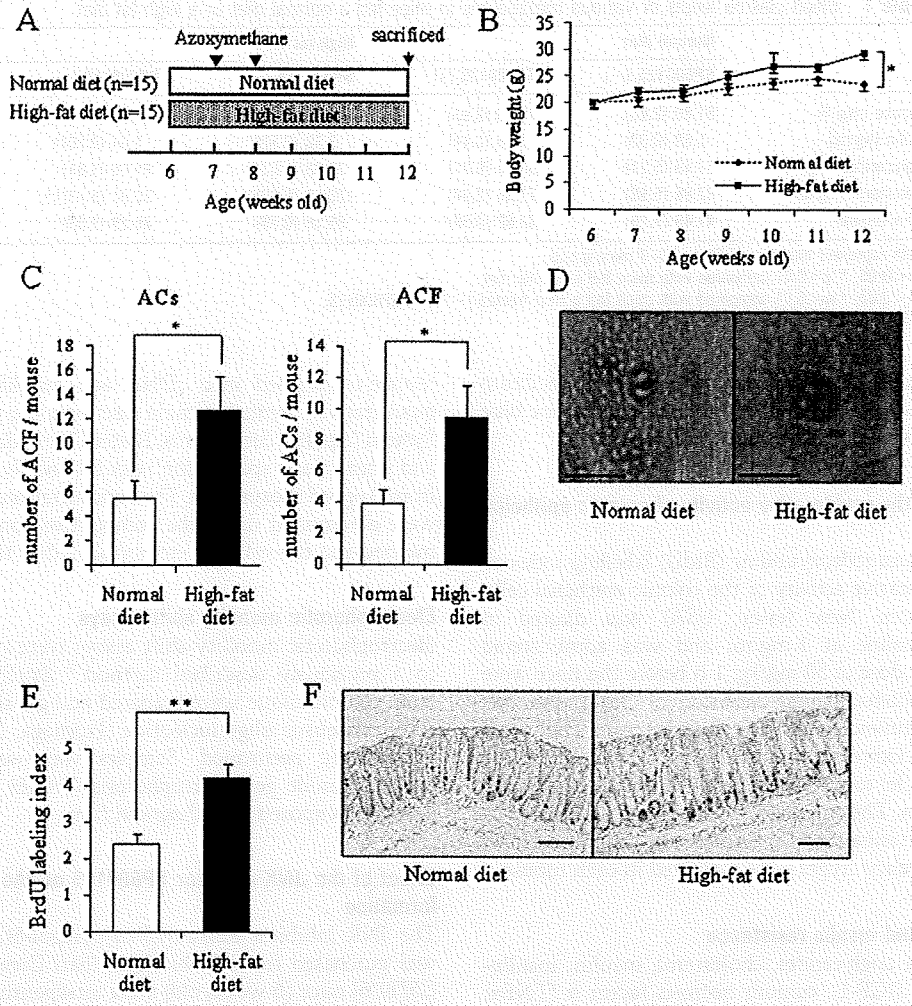

Figure 1 Enhanced proliferative activity of colonic epithelial cells in the presence of a high-fat diet. (A) ACF experiment protocol. Mice (6 weeks old) were divided into a normal diet group (n = 15) and a high-fat diet group (n = 15). Mice in each group were given two weekly intraperitoneal injections of 10 mg/kg of AOM. Six weeks after the start of the normal diet or high-fat diet, the mice were killed. (B) Changes in the body weights of mice fed a normal diet (broken line, n = 15) and mice fed a high-fat diet (solid line, n = 15) and treated with AOM. *Significant differences were observed between the normal diet and high-fat diet groups at all time points except for the initial measurement. *$p<0.01$. (C) Average numbers of ACs and ACF for mice fed a normal diet (n = 9) and mice fed a high-fat diet (n = 9). Each column represents the mean with the SEM; *$p<0.05$. (D) Stereomicroscopic observations of ACF in colon specimens from each group. Samples were stained with 0.2% methylene blue. Scale bar: 100 μm. (E) Average BrdU labelling index in each group in the ACF formation experiment. BrdU was administered intraperitoneally 1 h before the mice were killed. Both indices were expressed as the percentage of positively stained nuclei to the total number of nuclei counted in the crypts of the colon. Each bar represents the mean with the SEM of 9 mice/group. **$p<0.01$. (F) Representative immunohistochemical staining for BrdU in each group. Scale bar: 100 μm. ACs, aberrant crypts; ACF, aberrant crypt foci; AOM, azoxymethane; BrdU, 5-bromodeoxyuridine.

have demonstrated that colonic tumours of human origin exhibit an elevated expression of JNK/c-Jun.[22 25] However, the involvement of the JNK/c-Jun pathway in colon carcinogenesis under a HFD condition has not been previously reported.

Therefore, in this study, we investigated the activity of the insulin signalling pathway and the functional role of the JNK/c-Jun pathway in colorectal carcinogenesis and epithelial cell proliferation in the presence of hyperinsulinaemia induced by a HFD. This novel mechanism may explain the involvement of the JNK/c-Jun pathway in the effect of dietary fat intake on colon carcinogenesis.

MATERIALS AND METHODS

Animals and diets

C57Bl/6J mice were purchased from CLEA Japan (Tokyo, Japan). The animals were fed, either a normal diet (ND) or a HFD until the end of the study. The compositions of the ND (MF; Oriental Yeast Co., Tokyo, Japan) and the HFD (High Fat Diet 32; CLEA Japan, Tokyo, Japan) have been previously described.[12] Three to five mice were housed per metallic cage, with sterilised softwood chips used as bedding, in a barrier-sustained animal room air-conditioned at 24 (SD 2) °C and 55% humidity under a 12 h light/dark cycle.

Analysis of aberrant crypt foci

Six-week-old male mice were divided into a ND group and a HFD group. Mice in each group were given two weekly intraperitoneal injections of 10 mg/kg of azoxymethane (AOM) (Sigma, St. Louis, Missouri, USA) and were killed at 6 weeks following the initiation of AOM injection (fig 1A). The entire colon was removed, gently flushed with saline to remove any faecal contents, opened longitudinally, and fixed in 10% neutralised formalin; the numbers of ACF and aberrant crypts

Table 1 Blood plasma levels of various metabolites in mice fed a normal diet or a high-fat diet

	Normal diet		High-fat diet	
	SP600125 (−)	SP600125 (+)	SP600125 (−)	SP600125 (+)
Glucose (mg/dl)	81.80 (2.20)	76.50 (2.93)	180.00 (9.63)**	143.00 (10.54)†
Insulin (ng/ml)	1.69 (0.32)	1.96 (0.44)	3.38 (0.52)*	1.54 (0.50)†
Triglycerides (mg/dl)	57.43 (5.21)	55.00 (6.21)	77.68 (10.31)	61.66 (5.81)
Cholesterol (mg/dl)	87.86 (5.96)	77.85 (2.94)	120.14 (5.62)*	92.97 (5.43)††
TNFα (pg/ml)	41.49 (7.19)	32.62 (0.64)	36.18 (0.75)	35.29 (2.03)

Data represent the mean (SEM) of 6–9 mice/group.
*p<0.05, **p<0.01 compared with mice fed a normal diet.
†p<0.05, ††p<0.01 compared with mice fed a HFD treated (−) with SP600125.
TNFα, tumour necrosis factor α

(ACs) were then counted as described previously.[24] To facilitate the counting, the colons were stained with 0.2% methylene blue solution and were observed using stereomicroscopy.

Assay for assessing the proliferative activity of colonic epithelial cells

We evaluated the 5-bromodeoxyuridine (BrdU) labelling index to determine the proliferative activity of the colonic epithelial cells. BrdU (BD Biosciences, New Jersey, USA) was diluted in phosphate-buffered saline at 1 mg/ml and was administered intraperitoneally at a dose of 50 mg/kg, 1 h before the mice were killed. The immunohistochemical detection of BrdU was performed using a commercial kit (BD Biosciences). The BrdU labelling index was expressed as the ratio of the number of positively stained nuclei to the total number of nuclei counted in the crypts of the colon. The criteria for crypt selection included the presence of a clearly visible and continuous cell column on each side of the crypt. Twenty crypts were evaluated in each mouse.

Plasma lipid levels and insulin resistance

The levels of plasma triglycerides, cholesterol, insulin, insulin-like growth factor-1 (IGF-1), tumour necrosis factor α (TNFα) and blood glucose were measured using a WAKO enzyme-linked immunosorbent assay (ELISA) kit (Wako Pure Chemical, Osaka, Japan) (n = 10 from each group). We measured the plasma concentrations of triglycerides and cholesterol according to the manufacturer's instructions.

Immunoblotting

The extracted protein was separated using sodium dodecylsulfate polyacrylamide gel electrophoresis (SDS-PAGE) and the separated proteins were transferred to a polyvinylidene difluoride (PVDF) membrane (Amersham, London, UK). The membranes were probed with primary antibodies specific for phospho-JNK, JNK, phospho-extracellular signal regulated kinase (ERK), ERK, phospho-p38 MAPK, p38 MAPK, phospho-c-Jun, c-Jun, phospho-insulin receptor substrate-1 (IRS-1) (Ser307), IRS-1, phospho-Akt (Ser473), Akt, phospho-mammalian target of rapamycin (mTOR), mTOR, phospho-p70 ribosomal S6 kinase (S6K), S6K (Cell Signalling Technology, Danvers, Massachusetts, USA) and glyceraldehyde-3-phosphate dehydrogenase (GAPDH) (Trevigen, Gaithersburg, Maryland, USA). Horseradish-peroxidase-conjugated secondary antibodies and the ECL detection kit (Amersham) were used for the detection of specific proteins.

Gene expression analysis

Total RNA was extracted from the colonic epithelium using the RNeasy Mini Kit (Qiagen, Hilden, Germany). For real-time reverse transcription polymerase chain reaction, total RNA was reverse-transcribed into cDNA and amplified using real-time quantitative polymerase chain reaction using the ABI PRISM 7700 System (Applied Biosystems, Foster City California, USA). Probes and primer pairs specific for *cyclin D1* and *β-actin* were purchased from Applied Biosystems. The concentrations of the target genes were determined using the competitive computed tomography method and the values were normalised to the internal control.

Electrophoretic mobility shift assays

Electrophoretic mobility shift assays were performed according to a previously described method.[25] Briefly, nuclear extracts from colonic tissue were prepared and gel shift assays using an AP-1 consensus oligonucleotide (Promega, Madison, Wisconin, USA) were performed. Samples were separated using 4% polyacrylamide gel electrophoresis (PAGE), and the gels were dried and exposed to radiograph film.

Effect of the JNK inhibitor SP600125 on the induction of ACF formation

The JNK inhibitor anthra[1,9-*cd*]pyrazol-6(2*H*)-one (SP600125) was purchased from Calbiochem (San Diego, Calfornia, USA). C57Bl/6J mice (6 weeks old) were intraperitoneally injected with SP600125 (10 or 50 mg/kg) or vehicle (5% dimethyl sulfoxide (DMSO), 20% Cremophor EL, 75% saline) daily until the end of the experiment. The mice were fed the ND or the HFD and received AOM injections according to the ACF protocol.

Statistical analysis

Statistical analyses of the number of ACF, the BrdU labelling index, and the blood test results were conducted using the Mann–Whitney U test. Other statistical analyses were performed using the Student t test. Values of $p<0.05$ were regarded as denoting statistical significance.

RESULTS

Enhanced formation of aberrant crypt foci and increase in the cell proliferative activity in mice fed a high-fat diet

To examine the effect of a HFD on the promotion of colonic epithelial cell proliferation, the formation of chemically induced ACF (defined as clusters of ACs) was examined in the colon specimens as a marker of early stage colorectal carcinogenesis.[26 27] The proliferative activity of the colonic epithelial cells was also determined using the BrdU labelling index. The ACF experimental protocol is shown in fig 1A. The numbers of ACF and ACs were significantly higher in mice fed a HFD than in those fed a ND (fig 1C). The macroscopic characteristics of the ACF in the ND and HFD groups are shown in fig 1D; no morphological differences in the ACF were observed between the ND and the HFD groups. Furthermore, a significant increase

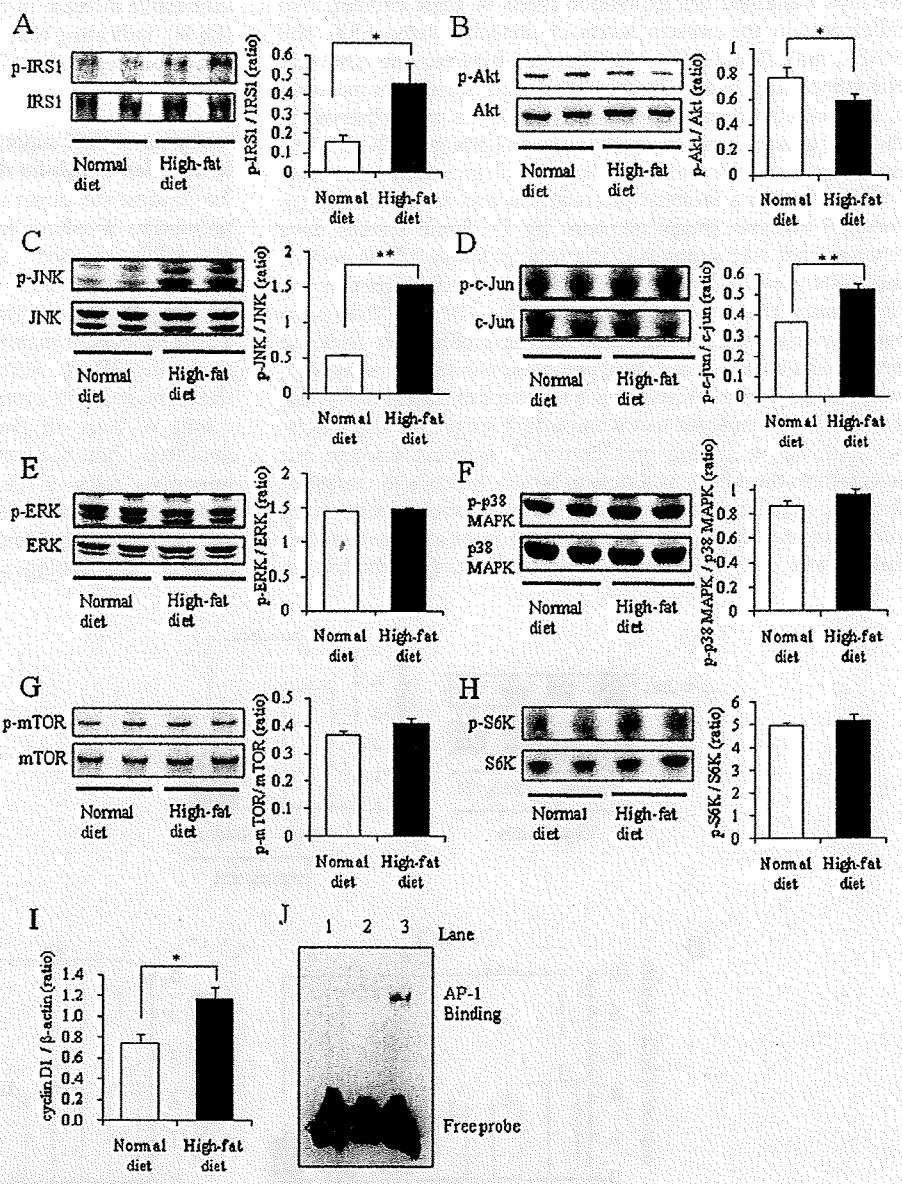

Figure 2 JNK activity and the signalling pathways for both insulin resistance and cell proliferation. A western blot analysis for phosphorylated and total IRS-1 (A), Akt (B), JNK (C), c-Jun (D), ERK (E), p38 MAPK (F), mTOR (G) and S6K (H) in colon specimens from mice fed a normal diet (n = 5) and mice fed a high-fat diet (n = 5). Representative western blotting images are shown. Right panel: graphs showing the ratios of the phosphorylated protein level to the total protein level. (I) Real time reverse transcription polymerase chain reaction analysis for the gene expression of *cyclin D1* in colon specimens from mice fed a normal diet (n = 6) and mice fed a high-fat diet (n = 6). Each column represents the mean with the SEM; *p<0.05, **p<0.01. (J) Electromobility shift assay autoradiogram shows the marked induction of AP-1 DNA binding under high-fat diet conditions. Lane 1, free probe alone (no nuclear extracts); lane 2, normal diet; lane 3, high-fat diet. ERK, extra-cellular signal-related kinase; IRS-1, insulin receptor substrate-1; JNK, c-Jun N-terminal kinase; MAPK, mitogen-activated protein kinase; mTOR, mammalian target of rapamycin; S6K, p70 ribosmal S6 kinase.

in the BrdU index was observed in the HFD group, compared with in the ND group (fig 1E,F). These results indicate that the proliferative activity of the colonic epithelial cells was promoted by the HFD, resulting in an increase in the number of ACF.

The body weights were significantly higher in the HFD group than in the ND group after 1 week of treatment (that is, at 7 weeks of age), and this difference was maintained until the end of the study (fig 1B). We next investigated the blood plasma levels of various metabolites in the ND and HFD groups. The levels of fasting plasma glucose, insulin, TNFα, lipids and IGF-1 were measured and are shown in table 1 and supplementary fig 1. Compared with the ND group, the HFD group had significantly higher fasting plasma glucose, insulin cholesterol and IGF-1 levels. Meanwhile, the plasma TNFα and triglyceride levels were not significantly different between the two groups.

The JNK pathway is activated in the colonic epithelium of mice fed a high-fat diet

To clarify the mechanisms underlying the enhanced proliferative activity of the colonic epithelial cells in the HFD group, we investigated the expression levels of various potential target proteins in colon specimens prepared from the ND and HFD groups. Because the plasma insulin level was significantly increased in the HFD group, we first speculated that an insulin signalling pathway downstream of the insulin receptor, such as the PI3K/Akt signalling pathway, might be involved in the promotion of colonic epithelial cell proliferation in the presence of a HFD. Akt plays an important role in a variety of biological processes including cell survival, cell growth, and oncogenesis[28] and is activated by insulin via the phosphorylation of IRS-1.[29] Surprisingly, the results of a western blot analysis revealed that the amount of phosphorylated Akt was lower in the HFD group than in the ND group (fig 2B). However, a significant increase in the level of phosphorylated IRS-1 was observed in the HFD group, compared with in the ND group (fig 2A). These results imply the existence of insulin resistance in the colonic epithelium. The phosphorylation of IRS-1 has emerged as a key event in insulin resistance.[30] Indeed, a large number of protein kinases have been shown to cause the phosphorylation of IRS-1, including JNK,[31] ERK,[32] mTOR,[33] and S6K.[34] Therefore,

we next examined the expression levels of these proteins. No differences in the protein levels of phosphorylated ERK, p38 MAPK, mTOR and S6K were observed between the HFD and ND groups (fig 2E–H). On the other hand, significant increases in the levels of phosphorylated JNK and c-Jun were observed in the HFD group, compared with in the ND group (fig 2C,D). The expressions of JNK and c-Jun in the colonic epithelium were confirmed using a western blot analysis and an immunohistochemical analysis (supplementary fig 2). Some studies have reported that Akt suppresses the JNK pathway.[35 36] Moreover, the mRNA level of cyclin D1 was significantly higher in the HFD group than in the ND group (fig 2I). The JNK/c-Jun pathway is a critical component of the proliferative response and induces G0 to G1 cell cycle progression in many cell types;[37] furthermore, cyclin D1, which is a regulator of the G1 to S phase transition, has emerged as an important target for the JNK/c-Jun pathway in driving proliferation.[35] We next directed our attention to the AP-1 transcription factor, which is the target of the JNK signalling pathway and, as mentioned earlier, is an important transcription factor involved in oncogenic transformation and cell proliferation. Our data clearly indicated an impressive increase in the activation of AP-1 in the HFD group (fig 2J), indicating that the JNK/c-Jun pathway was activated in the colonic epithelia of these animals.

Inhibition of JNK suppresses colonic epithelial cell proliferation in mice fed a high-fat diet

To confirm the direct involvement of the JNK pathway in the promotion of colonic epithelial cell proliferation in the presence of a HFD, we used a specific JNK inhibitor, SP600125, in the ACF experiment. ACF formation and the BrdU labelling index were significantly suppressed by SP600125 in the HFD group in a dose dependent manner, but no effect was observed in the ND group (fig 3B–D). Furthermore, the JNK inhibitor attenuated the increase in the protein levels of phosphorylated c-Jun in the colons of mice in the HFD group (fig 3A). These results indicated that the activation of the JNK pathway played important roles in the increase in epithelial cell proliferation observed in the mice fed a HFD and might play an important role in promoting colonic epithelial cell proliferation in mice fed a HFD. The fasting plasma glucose, insulin and cholesterol

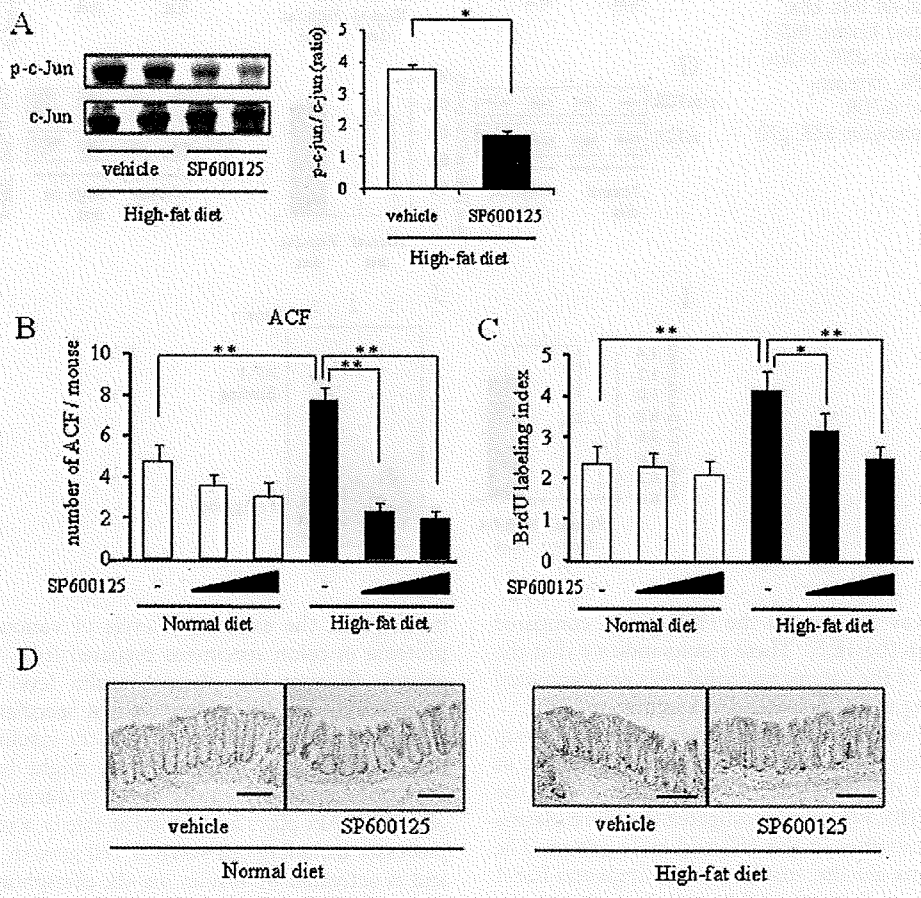

Figure 3 Suppression of colonic epithelial cell hyper-proliferation by JNK inhibitor in the presence of a high-fat diet. Mice (6 weeks old) were fed a normal diet or a high-fat diet and were injected intraperitoneally with the JNK inhibitor, SP600125 (10 or 50 mg/kg) or with the vehicle only daily until the end of the experiment. The mice in each group were also given two weekly intraperitoneal injections of 10 mg/kg of AOM. (A) Western blot analysis of phosphorylated and total c-Jun in colon specimens from mice treated (+) or not treated (−) with SP600125. Right panel: graphs showing the ratios of the phosphorylated protein levels to the total protein levels. Each column represents the mean with the SEM of 6 mice/group; *$p<0.05$, compared with mice treated (−) with SP600125. (B) Average numbers of ACF in the mice fed a normal diet and the mice fed a high-fat diet treated (+) or not treated (−) with SP600125. Each column represents the mean with the SEM of 6 mice/group; **$p<0.01$. (C) The average BrdU labelling index decreased in mice fed a high-fat diet in a dose dependent manner, but not in mice fed a normal diet. Each column represents the mean with the SEM of 6 mice/group; *$p<0.05$, **$p<0.01$. (D) Representative immunohistochemical staining for BrdU in each group. Scale bar: 100 μm. ACF, aberrant crypt foci; AOM, azoxymethane; BrdU, 5-bromodeoxyuridine; JNK, c-Jun N-terminal kinase.

levels were significantly reduced by SP600125 in the HFD group, but no effect was observed in the ND group (table 1). The plasma TNFα and triglyceride levels after treatment with SP600125 were similar between the two groups.

DISCUSSION

Previous studies have provided evidence of an association between dietary fat intake and an increased risk of colorectal carcinogenesis,[2 4] but the molecular mechanisms underlying the promotion of colorectal carcinogenesis by a HFD remain unclear. In the present study, we showed a significant enhancement in the formation of ACF and an increase in the proliferative activity of the colonic epithelial cells in the HFD group, compared with in the ND group. Additionally, we demonstrated the activation of the JNK/c-Jun pathway and the inactivation of Akt in colonic epithelial cells in the HFD group. Furthermore, a JNK specific inhibitor significantly suppressed the increase in epithelial cell proliferation only in the HFD group, suggesting that JNK/c-Jun may play an important role in promoting colorectal carcinogenesis and epithelial cell proliferation in the presence of a HFD.

Animal models exhibiting high-fat-induced hyperinsulinaemia provide a unique opportunity to explore the potential molecular mechanisms underlying the promotion of colorectal carcinogenesis and epithelial cell proliferation by a HFD. Insulin is now known to be an important growth factor for colonic epithelial cells,[7 8] and the insulin receptor has been detected in normal colorectal epithelium and cancer tissue.[58] The insulin-signal transduction pathway can be mediated by the activation of IRS-1/PI3K/Akt signalling and is involved in the regulation of gene expression and mitogenicity. Therefore, we first speculated that PI3K/Akt activation might be involved in the promotion of colonic cell proliferation in the presence of a HFD because the plasma insulin level was elevated in the HFD group. However, our results surprisingly showed that the Akt activity was decreased in the HFD group compared with in the ND group, whereas a significant increase in the level of phosphorylated IRS-1 was observed in the HFD group, compared with in the ND group. These results suggested that, in vivo, HFD induced insulin resistance in the colonic epithelium, causing the inhibition of PI3K/Akt signalling (supplementary fig 3). These molecular mechanisms of insulin resistance have been studied in the liver and adipose tissues of various models of diabetes,[13] with results that are compatible with the presently reported results. Thus, we next examined signalling pathways involved in both insulin resistance and proliferation, including the JNK pathway.

We observed an increased in JNK/c-Jun activity in colonic epithelial cells from the HFD group. Therefore, we investigated the effect of SP600125, a specific JNK inhibitor, on the colonic epithelium to determine the direct involvement of JNK activation in colon carcinogenesis and epithelial proliferation under a HFD condition. The inhibition of JNK activation reportedly improves insulin resistance.[59] Our results indeed demonstrated that SP600125 attenuated the blood glucose and plasma insulin levels, suggesting that this inhibitor might suppress colonic epithelial cell proliferation in the presence of a HFD via some indirect effects, such as the amelioration of insulin resistance. However, a western blot analysis for colonic epithelial protein in the HFD group clearly showed the attenuation of JNK activity after treatment with SP600125. Furthermore, the increase in ACF formation and the BrdU labelling index were distinctly restored by SP600125 in the HFD. Therefore, these results imply that insulin resistance and the promotion of colonic epithelial proliferation in the presence of a HFD occur via independent mechanisms. Our data strongly suggest that a HFD promotes the JNK/c-Jun pathway, resulting in the promotion of cell proliferative activity and, consequently, the promotion of colon carcinogenesis.

We also investigated the activation of the mTOR/S6K pathway in colonic epithelial cells to elucidate the involvement of this pathway in cell proliferation in the presence of a HFD. The important role of mTOR in mammalian cells is related to its control of mRNA translation. The targets for mTOR signalling are proteins involved in the control of the translational machinery; these targets include S6K, which regulates the initiation and elongation phases of translation.[40] Regarding upstream control, mTOR is regulated by signalling pathways linked to several oncoproteins or tumour suppressors.[41] Recently, the mTOR/S6K pathway, which is similar to the JNK pathway, has emerged as a critical signalling pathway in the development of insulin resistance.[42] Although the excess nutrient levels associated with an obese state can lead to the activation of mTOR/S6K and the desensitisation of insulin signalling,[42] we found no differences in the colonic epithelial protein levels of phosphorylated mTOR and S6K between the HFD and ND groups in the present study. Furthermore, we previously reported that treatment with rapamycin, an mTOR specific inhibitor, did not reduce the BrdU labelling index or ACF formation in mice fed a HFD.[12] These results indicate that the activation of the mTOR pathway may not play an important role in the increase in colonic epithelial cell proliferation in the presence of a HFD condition (supplementary fig 4).

Adipocytokines, such as free fatty acid and tumour necrosis factor α, have been reported to be potent JNK activators,[15 43] although the molecular pathways involved in their action remain unclear. Several studies have demonstrated that transforming growth factor β (TGFβ) regulates the JNK signalling pathway.[44] TGFβs are known to act as inhibitors of cell proliferation;[45] recently, however, the elevated expression of TGFβs has been suggested to be responsible for oncogenesis.[46] Raju *et al*[47] showed that TGFβs were upregulated in colonic tumours and a select subset of ACF and that dietary fat modulated TGFβ expression in colonic tumours and mucosae. In the present study, however, the expression levels of TGFβs in the colonic epithelium were not elevated in the HFD group (data not shown). Further studies are warranted to investigate whether the JNK signalling pathway via TGFβ might play an important role in colon carcinogenesis and epithelial proliferation under a HFD condition.

This study presents a novel mechanism explaining the involvement of the JNK pathway in the effect of dietary fat intake on colorectal carcinogenesis and epithelial cell proliferation. Importantly, JNK activation was associated with the promotion of colonic cell proliferative activity only in the presence of a HFD, but not in the presence of a ND. At present, an elevated plasma insulin level is thought to possibly enhance the proliferative state through the activation of an insulin signalling pathway downstream of the insulin receptor, such as the PI3K/Akt signalling pathway, in the colon.[10] Currently, however, in vivo mechanistic evidence has confirmed this hypothesis to be insufficient.[45] Our in vivo results suggested that a HFD induced insulin resistance and an abnormally elevated level of JNK activity in the colonic epithelial and that the activated JNK pathway promoted colorectal epithelial cell proliferation. This study therefore demonstrated that JNK activation is one of several possible mechanisms underlying the promotion of colonic cell proliferative activity and the early

stage of colon carcinogenesis in the presence of a HFD. We propose that JNK/c-Jun may be a novel therapeutic target for the prevention of colorectal cancer in obese populations consuming a HFD. In the future, continued investigations are needed to elucidate the JNK activators and the precise role of JNK activation in the process of colorectal carcinogenesis under the HFD conditions.

Acknowledgements: We thank M Hiraga for her technical assistance.

Funding: This work was supported in part by a Grant-in-Aid for research on the Third Term Comprehensive Control Research for Cancer from the Ministry on Health, Labor and Welfare, Japan, to AN; a grant from the National Institute of Biomedical Innovation (NBIO) to AN; a grant from the Ministry of Education, Culture, Sports, Science and Technology, Japan (KIBAN-B), to AN; and a grant program "Collaborative Devlopment of Innovative Seeds" from the Japan Science and Technology Agency (JST).

Competing interests: None.

Ethics approval: All animal experiments were approved by the Institutional Animal Care and Use Committee of Yokohama City University School of Medicine.

Provenance and peer review: Not commissioned; externally peer reviewed.

REFERENCES

1. **Jemal A,** Siegel R, Ward E, *et al*. Cancer statistics, 2008. *CA Cancer J Clin* 2008;**58**:71–96.
2. **Giovannucci E,** Goldin B. The role of fat, fatty acids, and total energy intake in the etiology of human colon cancer. *Am J Clin Nutr* 1997;**66**:1564S–71S.
3. **Friedenreich CM,** Orenstein MR. Physical activity and cancer prevention: etiologic evidence and biological mechanisms. *J Nutr* 2002;**132**:3456S–64S.
4. **Giovannucci E,** Willett WC. Dietary factors and risk of colon cancer. *Ann Med* 1994;**26**:443–52.
5. **Lasko CM,** Bird RP. Modulation of aberrant crypt foci by dietary fat and caloric restriction: the effects of delayed intervention. *Cancer Epidemiol Biomarkers Prev* 1995;**4**:49–55.
6. **Rao CV,** Hirose Y, Indranie C, *et al*. Modulation of experimental colon tumorigenesis by types and amounts of dietary fatty acids. *Cancer Res* 2001;**61**:1927–33.
7. **Giovannucci E.** Insulin, insulin-like growth factors and colon cancer: a review of the evidence. *J Nutr* 2001;**131**:3109S–20S.
8. **Corpet DE,** Jacquinet C, Peiffer G, *et al*. Insulin injections promote the growth of aberrant crypt foci in the colon of rats. *Nutr Cancer* 1997;**27**:316–20.
9. **Tran TT,** Medline A, Bruce WR. Insulin promotion of colon tumors in rats. *Cancer Epidemiol Biomarkers Prev* 1996;**5**:1013–5.
10. **Tran TT,** Naigamwalla D, Oprescu AI, *et al*. Hyperinsulinemia, but not other factors associated with insulin resistance, acutely enhances colorectal epithelial proliferation in vivo. *Endocrinology* 2006;**147**:1830–7.
11. **Aparicio T,** Kotelevets L, Tsocas A, *et al*. Leptin stimulates the proliferation of human colon cancer cells in vitro but does not promote the growth of colon cancer xenografts in nude mice or intestinal tumorigenesis in Apc(Min/+) mice. *Gut* 2005;**54**:1136–45.
12. **Fujisawa T,** Endo H, Tomimoto A, *et al*. Adiponectin suppresses colorectal carcinogenesis under the high-fat diet condition. *Gut* 2008;**57**:1531–8.
13. **Hirosumi J,** Tuncman G, Chang L, *et al*. A central role for JNK in obesity and insulin resistance. *Nature* 2002;**420**:333–6.
14. **Solinas G,** Naugler W, Galimi F, *et al*. Saturated fatty acids inhibit induction of insulin gene transcription by JNK-mediated phosphorylation of insulin-receptor substrates. *Proc Natl Acad Sci USA* 2006;**103**:16454–9.
15. **Davis RJ.** Signal transduction by the JNK group of MAP kinases. *Cell* 2000;**103**:239–52.
16. **Karin M,** Liu Z, Zandi E. AP-1 function and regulation. *Curr Opin Cell Biol* 1997;**9**:240–6.
17. **Yang YM,** Bost F, Charbono W, *et al*. C-Jun NH(2)-terminal kinase mediates proliferation and tumor growth of human prostate carcinoma. *Clin Cancer Res* 2003;**9**:391–401.
18. **Gross ND,** Boyle JO, Du B, *et al*. Inhibition of Jun NH2-terminal kinases suppresses the growth of experimental head and neck squamous cell carcinoma. *Clin Cancer Res* 2007;**13**:5910–7.
19. **Hideshima T,** Hayashi T, Chauhan D, *et al*. Biologic sequelae of c-Jun NH(2)-terminal kinase (JNK) activation in multiple myeloma cell lines. *Oncogene* 2003;**22**:8797–801.
20. **Mingo-Sion AM,** Marietta PM, Koller E, *et al*. Inhibition of JNK reduces G2/M transit independent of p53, leading to endoreduplication, decreased proliferation, and apoptosis in breast cancer cells. *Oncogene* 2004;**23**:596–604.
21. **Nateri AS,** Spencer-Dene B, Behrens A. Interaction of phosphorylated c-Jun with TCF4 regulates intestinal cancer development. *Nature* 2005;**437**:281–5.
22. **Hardwick JC,** van den Brink GR, Offerhaus GJ, *et al*. NF-kappaB, p38 MAPK and JNK are highly expressed and active in the stroma of human colonic adenomatous polyps. *Oncogene* 2001;**20**:819–27.
23. **Wang H,** Birkenbach M, Hart J. Expression of Jun family members in human colorectal adenocarcinoma. *Carcinogenesis* 2000;**21**:1313–7.
24. **Osawa E,** Nakajima A, Wada K, *et al*. Peroxisome proliferator-activated receptor gamma ligands suppress colon carcinogenesis induced by azoxymethane in mice. *Gastroenterology* 2003;**124**:361–7.
25. **Boussiotis VA,** Freeman GJ, Taylor PA, *et al*. p27kip1 functions as an anergy factor inhibiting interleukin 2 transcription and clonal expansion of alloreactive human and mouse helper T lymphocytes. *Nat Med* 2000;**6**:290–7.
26. **McLellan EA,** Bird RP. Aberrant crypts: potential preneoplastic lesions in the murine colon. *Cancer Res* 1988;**48**:6187–92.
27. **Konstantakos AK,** Siu IM, Pretlow TG, *et al*. Human aberrant crypt foci with carcinoma in situ from a patient with sporadic colon cancer. *Gastroenterology* 1996;**111**:772–7.
28. **Testa JR,** Bellacosa A. AKT plays a central role in tumorigenesis. *Proc Natl Acad Sci USA* 2001;**98**:10983–5.
29. **Datta SR,** Brunet A, Greenberg ME. Cellular survival: a play in three Akts. *Genes Dev* 1999;**13**:2905–27.
30. **Zick Y.** Insulin resistance: a phosphorylation-based uncoupling of insulin signaling. *Trends Cell Biol* 2001;**11**:437–41.
31. **Aguirre V,** Werner ED, Giraud J, *et al*. Phosphorylation of Ser307 in insulin receptor substrate-1 blocks interactions with the insulin receptor and inhibits insulin action. *J Biol Chem* 2002;**277**:1531–7.
32. **De Fea K,** Roth RA. Modulation of insulin receptor substrate-1 tyrosine phosphorylation and function by mitogen-activated protein kinase. *J Biol Chem* 1997;**272**:31400–6.
33. **Ozes ON,** Akca H, Mayo LD, *et al*. A phosphatidylinositol 3-kinase/Akt/mTOR pathway mediates and PTEN antagonizes tumor necrosis factor inhibition of insulin signaling through insulin receptor substrate-1. *Proc Natl Acad Sci USA* 2001;**98**:4640–5.
34. **Um SH,** D'Alessio D, Thomas G. Nutrient overload, insulin resistance, and ribosomal protein S6 kinase 1, S6K1. *Cell Metab* 2006;**3**:393–402.
35. **Park HS,** Kim MS, Huh SH, *et al*. Akt (protein kinase B) negatively regulates SEK1 by means of protein phosphorylation. *J Biol Chem* 2002;**277**:2573–8.
36. **Brazil DP,** Park J, Hemmings BA. PKB binding proteins. Getting in on the Akt. *Cell* 2002;**111**:293–303.
37. **Shaulian E,** Karin M. AP-1 in cell proliferation and survival. *Oncogene* 2001;**20**:2390–400.
38. **Kiunga GA,** Raju J, Sabljic N, *et al*. Elevated insulin receptor protein expression in experimentally induced colonic tumors. *Cancer Lett* 2004;**211**:145–53.
39. **Kaneto H,** Nakatani Y, Miyatsuka T, *et al*. Possible novel therapy for diabetes with cell-permeable JNK-inhibitory peptide. *Nat Med* 2004;**10**:1128–32.
40. **Avruch J,** Belham C, Weng Q, *et al*. The p70 S6 kinase integrates nutrient and growth signals to control translational capacity. *Prog Mol Subcell Biol* 2001;**26**:115–54.
41. **Guertin DA,** Sabatini DM. Defining the role of mTOR in cancer. *Cancer Cell* 2007;**12**:9–22.
42. **Um SH,** Frigerio F, Watanabe M, *et al*. Absence of S6K1 protects against age- and diet-induced obesity while enhancing insulin sensitivity. *Nature* 2004;**431**:200–5.
43. **Chang L,** Karin M. Mammalian MAP kinase signalling cascades. *Nature* 2001;**410**:37–40.
44. **Wang W,** Zhou G, Hu MC, *et al*. Activation of the hematopoietic progenitor kinase-1 (HPK1)-dependent, stress-activated c-Jun N-terminal kinase (JNK) pathway by transforming growth factor beta (TGF-beta)-activated kinase (TAK1), a kinase mediator of TGF beta signal transduction. *J Biol Chem* 1997;**272**:22771–5.
45. **Roberts AB,** Anzano MA, Wakefield LM, *et al*. Type beta transforming growth factor: a bifunctional regulator of cellular growth. *Proc Natl Acad Sci USA* 1985;**82**:119–23.
46. **Wakefield LM,** Roberts AB. TGF-beta signaling: positive and negative effects on tumorigenesis. *Curr Opin Genet Dev* 2002;**12**:22–9.
47. **Raju J,** McCarthy B, Bird RP. Steady state levels of transforming growth factor-beta1 and -beta2 mRNA and protein expression are elevated in colonic tumors in vivo irrespective of dietary lipids intervention. *Int J Cancer* 2002;**100**:635–41.
48. **Endo H,** Fujisawa T, Takahashi H, *et al*. Author response to GUT/2009/177535. *Gut* 2009;**58**:1169–70.

Haploinsufficiency and acquired loss of *Bcl11b* and *H2AX* induces blast crisis of chronic myelogenous leukemia in a transgenic mouse model

Akiko Nagamachi,[1] Norimasa Yamasaki,[2] Kazuko Miyazaki,[2] Hideaki Oda,[3] Masaki Miyazaki,[4] Zen-ichiro Honda,[5] Ryo Kominami,[6] Toshiya Inaba[1] and Hiroaki Honda[2,7]

Departments of [1]Molecular Oncology, [2]Developmental Biology, Research Institute of Radiation Biology and Medicine, Hiroshima University, Hiroshima; [3]Department of Pathology, Tokyo Womens' Medical University, Tokyo; [4]Department of Immunology, Graduate School of Biomedical Sciences, Hiroshima University, Hiroshima; [5]Department of Allergy and Rheumatology, Faculty of Medicine, Graduate School of Medicine, University of Tokyo, Tokyo; [6]Department of Molecular Genetics, Graduate School of Medical and Dental Sciences, Niigata University, Niigata, Japan

(Received February 3, 2009/Revised March 11, 2009/Accepted March 12, 2009/Online publication April 21, 2009)

Chronic myelogenous leukemia (CML) is a hematological malignancy that begins as indolent chronic phase (CP) but inevitably progresses to fatal blast crisis (BC). p210BCR/ABL, a chimeric protein with enhanced kinase activity, initiates CML CP, and additional genetic alterations account for progression to BC, but the precise mechanisms underlying disease evolution are not fully understood. In the present study, we investigated the possible contribution of dysfunction of Bcl11b, a zinc-finger protein required for thymocyte differentiation, and of H2AX, a histone protein involved in DNA repair, to the transition from CML CP to BC. For this purpose, we crossed CML CP-exhibiting *p210BCR/ABL* transgenic (*BA*$^{tg/-}$) mice with *Bcl11b* heterozygous (*Bcl11b*$^{+/-}$) mice and *H2AX* heterozygous (*H2AX*$^{+/-}$) mice. Interestingly, *p210BCR/ABL* transgenic, *Bcl11b* heterozygous (*BA*$^{tg/-}$*Bcl11b*$^{+/-}$) mice and *p210BCR/ABL* transgenic, *H2AX* heterozygous (*BA*$^{tg/-}$*H2AX*$^{+/-}$) mice frequently developed CML BC with T-cell phenotype and died in a short period. In addition, whereas p210BCR/ABL was expressed in all of the leukemic tissues, the expression of Bcl11b and H2AX was undetectable in several tumors, which was attributed to the loss of the residual normal allele or the lack of mRNA expression. These results indicate that Bcl11b and H2AX function as tumor suppressor and that haploinsufficiency and acquired loss of these gene products cooperate with p210BCR/ABL to develop CML BC. (*Cancer Sci* 2009; 100: 1219–1226)

Chronic myelogenous leukemia (CML) is a disorder of hematopoietic stem cells, characterized by excessive and uncontrolled proliferation of differentiated myeloid cells.[1–3] Clinically, CML undergoes two different stages.[1–3] In the initial stage, chronic phase (CP), the leukemic cells retain the ability to differentiate into mature granulocytes and are sensitive to conventional therapies. However, after several years' duration of CP, the disease inevitably accelerates and ultimately progresses to the terminal stage, blast crisis (BC), which exhibits aggressive proliferation of immature blast cells and is resistant to intensive therapies.[1–3]

The cytogenetic hallmark of CML CP is t(9;22)(q34;q11) (known as Philadelphia chromosome, Ph), which generates a *BCR–ABL* fusion gene encoding a 210-kDa chimeric protein (p210BCR/ABL).[1–3] p210BCR/ABL possesses a constitutively active tyrosine kinase activity, which plays an essential role in the initiation of the disease.[1–3] Although Ph is the unique and sole chromosomal abnormality in CP, additional and non-random chromosomal abnormalities are frequently observed in BC, indicating that secondary genetic events account for the disease progression.[1–3]

To understand the pathogenesis of the disease, it is necessary to establish animal models that express *p210BCR/ABL* and recapitulate the clinical course of CML. For this purpose, we generated transgenic mice expressing *p210BCR/ABL* under the control of the mouse *TEC* promoter.[4] The *p210BCR/ABL* transgenic (hereafter, designated as *BA*$^{tg/-}$) mice reproducibly exhibited a myeloproliferative disorder closely resembling human CML CP.[4] In addition, by crossing *BA*$^{tg/-}$ mice with *p53* heterozygous mice and *Dok-1/Dok-2* knockout mice, we showed that the loss of p53 and absence of Dok-1/Dok-2 accelerated the disease and caused CML BC.[5,6] Furthermore, by applying retroviral insertional mutagenesis to *BA*$^{tg/-}$ mice, we demonstrated that overexpression and enhanced kinase activity of p210BCR/ABL and altered expression of Notch1 contribute to CML BC.[7] These results demonstrated that the *BA*$^{tg/-}$ mouse is not only regarded as a model for CML CP, but is also useful for investigating the molecular mechanisms underlying the progression from CP to BC.

Chromosomal and molecular analyses have revealed that several mechanisms are implicated in this process, such as: (i) loss of tumor suppressor; (ii) differentiation arrest; and (iii) chromosomal instability.[3] Indeed, as an example of (i), we demonstrated that loss of p53 cooperates with p210BCR/ABL and induces CML BC.[5,6] In the present report, as candidate genes for (ii) and (iii), we chose *Bcl11b* (also known as *Rit1* and *Ctip2*), encoding a transcription factor required for thymocyte differentiation,[8] and *H2AX*, encoding a histone protein involved in DNA repair,[9] and examined the possible contribution that dysfunction of these gene produces for the disease progression of CML. For this purpose, we crossed *BA*$^{tg/-}$ mice with mice heterozygous for *Bcl11b* (*Bcl11b*$^{+/-}$) or *H2AX* (*H2AX*$^{+/-}$) and generated *BA*$^{tg/-}$*Bcl11b*$^{+/-}$ mice and *BA*$^{tg/-}$*H2AX*$^{+/-}$ mice. Interestingly, both types of double transgenic mouse frequently developed CML BC and died in a short period. The pathological, flow cytometric, molecular, and chromosomal analyses of the diseased mice are described.

Materials and Methods

Mice. *p210BCR/ABL* transgenic, *Bcl11b* heterozygous, and *H2AX* heterozygous mice were generated as described previously.[4,8,10] Crossing and genotyping of the mice were carried out as described previously.[5] All of the mice were kept according to the guidelines of the Institute of Laboratory Animal Science, Hiroshima University.

Pathological analysis. Autopsies were carried out on dead or moribund animals. Peripheral blood smears were stained with Wight-Giemsa. After gross examination, tissues were fixed in

[7]To whom correspondence should be addressed. E-mail: hhonda@hiroshima-u.ac.jp

doi: 10.1111/j.1349-7006.2009.01172.x